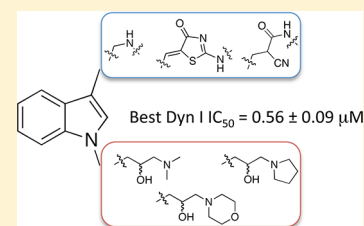


## Development of Second-Generation Indole-Based Dynamin GTPase Inhibitors

Christopher P. Gordon,<sup>†</sup> Barbara Venn-Brown,<sup>†</sup> Mark J. Robertson,<sup>†</sup> Kelly A. Young,<sup>†</sup> Ngoc Chau,<sup>‡</sup> Anna Mariana,<sup>‡</sup> Ainslie Whiting,<sup>‡</sup> Megan Chircop,<sup>‡</sup> Phillip J. Robinson,<sup>‡</sup> and Adam McCluskey<sup>\*,†</sup><sup>†</sup>Chemistry, Centre for Chemical Biology, School of Environmental and Life Sciences, The University of Newcastle, University Drive, Callaghan, NSW 2308, Australia<sup>‡</sup>Cell Signaling Unit and Cell Cycle Unit, Children's Medical Research Institute, The University of Sydney, 214 Hawkesbury Road, Westmead, NSW 2145, Australia

## S Supporting Information

**ABSTRACT:** Focused library development of our lead 2-cyano-3-(1-(3-(dimethylamino)propyl)-2-methyl-1H-indol-3-yl)-N-octylacrylamide (**2**) confirmed the tertiary dimethylamino-propyl moiety as critical for inhibition of dynamin GTPase. The cyanoamide moiety could be replaced with a thiazole-4(*SH*)-one isostere (**19**,  $IC_{50(dyn I)} = 7.7 \mu M$ ), reduced under flow chemistry conditions (**20**,  $IC_{50(dyn I)} = 5.2 \mu M$ ) or replaced by a simple amine. The latter provided a basis for a high yield library of compounds via a reductive amination by flow hydrogenation. Two compounds, **24** ( $IC_{50(dyn I)} = 0.56 \mu M$ ) and **25** ( $IC_{50(dyn I)} = 0.76 \mu M$ ), stood out. Indole **24** is nontoxic and showed increased potency against dynamin I and II in vitro and in cells ( $IC_{50(CME)} = 1.9 \mu M$ ). It also showed 4.4-fold selectivity for dynamin I. The indole **24** compound has improved isoform selectivity and is the most active in-cell inhibitor of clathrin-mediated endocytosis reported to date.



## INTRODUCTION

Dynamin is a large GTPase known to play a crucial role in membrane remodelling, notably during endocytosis.<sup>1</sup> Three dynamin genes exist, and while the expressed proteins have over 80% homology, they show differential tissue distribution, suggesting they may have distinct biological roles. Common to all are four domains, a GTPase domain (required for vesicle fission),<sup>2,3</sup> a pleckstrin homology domain (targeting domain and potentially a GTPase inhibitory module),<sup>4</sup> a bundle signaling element (which controls dynamin self-assembly into rings),<sup>5,6</sup> and a proline-rich domain (which interacts with proteins containing an SH3 domain<sup>2,4</sup> and is the site for dynamin phosphorylation in vivo).<sup>7,8</sup> Two crystal structures of mammalian dynamin I have been solved.<sup>9,10</sup> Each lack the PRD domain but provided insights into the complex dynamics involved in oligomerization and how dynamin may act as a scission protein in cells.

Endocytic mechanisms serve a variety of cellular functions including the uptake of cellular nutrients, regulation of cell-surface receptor expression and signaling, antigen presentation, and maintenance of synaptic transmission. Clathrin mediated endocytosis (CME) is one such mechanism and in mammalian cells its usual function is internalization of extracellular materials. In neuronal cells, this is a specialized pathway termed synaptic vesicle endocytosis (SVE) and its role is internalization of membrane to allow vesicle recycling.<sup>2,4</sup> SVE and CME thus perform distinct functional roles in different cell types but share the same underlying protein machinery.

The differences in SVE and CME mostly arise from which dynamin gene product is present. Dynamin II (dynII) is found

throughout the body and is the major scission protein for CME, while dynamin III (dynIII) is limited primarily to the brain and testes and at low levels in a few other tissues. The dynamin I (dynI) gene product is only found in neuronal cells where it coexists with the other two forms. DynI is expressed in these cells at about 50-fold higher levels compared with either dynIII or dynII. This high level of dynI was expected to be critical for neuronal cell function, however knockout studies have shown both dynII and especially dynIII are able to facilitate SVE with limited success, hinting to a range of redundancies within the endocytic network.<sup>11</sup> A crucial role has thus been suggested for dynI to allow SVE to occur across a broad range of neuronal activities and has been implicated as a potential target for epilepsy.<sup>1</sup>

Control of endocytic pathways presents immense therapeutic potential with defects in such pathways being involved in multiple disease states such as Alzheimer's disease, Huntington's disease, Stiff-person syndrome, Lewy body dementias, and Niemann–Pick type C disease.<sup>12–15</sup> Endocytic pathways are also utilized by viruses, including HIV,<sup>16</sup> and bacteria to gain entry into cells.<sup>17</sup> Links to genetic disease are also emerging with mutations in dynII causing Charcot–Marie–Tooth disease and centronuclear myopathy, and dynII mutations are involved in T-cell precursor acute lymphoblastic leukemia.<sup>18–20</sup> Recently attention has also turned toward nonendocytic roles that dynamin plays in the body including those involving the

Received: June 15, 2012

Published: November 20, 2012

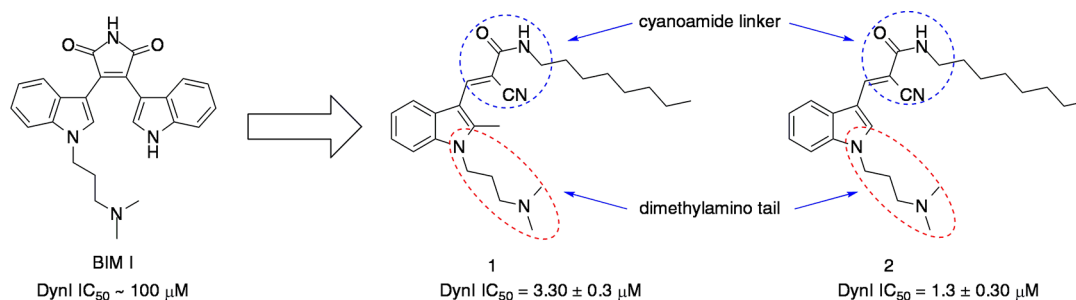
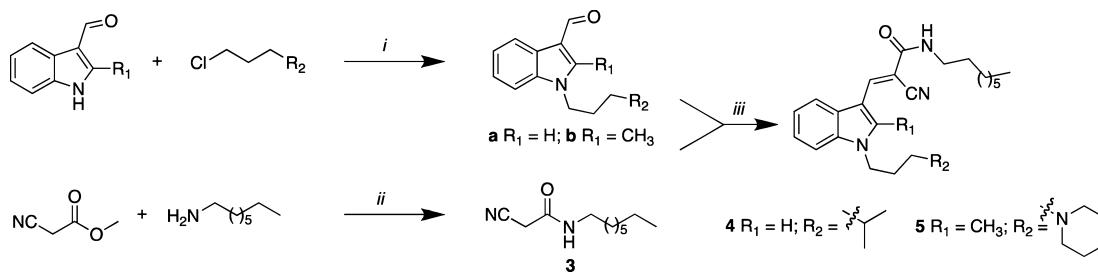


**Figure 1.** BIM I scaffold simplification for rational design of dynamin inhibitors which afforded indoles **1** and **2**.

### Scheme 1<sup>a</sup>



<sup>a</sup>Reagents and conditions: (i) NaH, THF, reflux, 72 h; (ii) MeOH, rt, 4 h; (iii) EtOH, microwave, 120 °C, 150 W, 20 min.

actin cytoskeleton, the sperm acrosome reaction, or cytokinesis.<sup>21–23</sup>

There is now a toolbox of dynamin inhibitors available, including the MiTMAB<sup>25</sup> Bis-T,<sup>26,27</sup> RTIL,<sup>28</sup> Iminiodyn,<sup>29</sup> Pthaladyn,<sup>30</sup> Dyngo,<sup>31</sup> and Rhodadyn<sup>32</sup> dynamin inhibitors. Within this palette perhaps the series displaying the most potential as therapeutic agents is a series of indole analogues (Figure 1).<sup>33</sup> The two most active of this series, indole **1** and indole **2**, display high cell permeability and efficacy with cellular IC<sub>50</sub> values less than an order of magnitude from the *in vitro* activity.<sup>33</sup> Indole **2** is nontoxic, with fibroblast cells remaining viable after 7 days.<sup>23,33</sup> Indole **2**, like MiTMAB, is a new class of antimetabolic agent with a novel mechanism of action, blocking cytokinesis specifically at the abscission stage. Our lead, **2**, induces cell death in cancer cells specifically following cytokinesis failure in dividing cells while nontumorigenic fibroblasts are much less sensitive.<sup>23</sup>

The indole-based dynamin inhibitors evolved from a series of bisindolylmaleimides (BIMs) via a focused compound library approach (Figure 1). Analogues in these initial libraries were decorated with relatively simple functional groups including cyclic and acyclic aliphatic hydrocarbons in addition to a number of benzyl moieties.<sup>33</sup> Given that these relatively simple alterations imparted a 100-fold increase in dynI inhibition potency, we sought to further explore this compound class and the potential to install more drug-like moieties in developing this second generation of indole-based dynamin inhibitors.

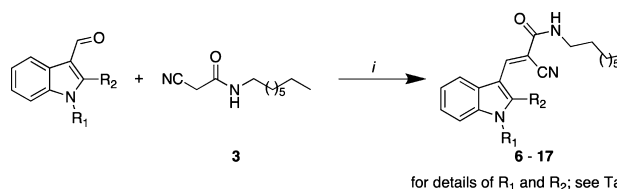
## RESULTS AND DISCUSSION

We have previously demonstrated that the dimethylamino moiety was a crucial element of the parent indole scaffold with shortening the tail from propyl to ethyl, resulting in a slight activity reduction while removal of the tail abolished inhibitory activity.<sup>33</sup> Given these limits, a more extensive investigation was proposed. Herein our initial focus was directed to the nitrogen atom of the dimethylamino tail with removal and increased shielding to be examined with the synthesis of compounds **4**

and **5** (Scheme 1). These were prepared via a three step procedure with alkylation of an indole (**a**, **b**), concurrent formation of the cyanoamide (**3**), followed by coupling via a Knoevenagel condensation.

Additional dimethylamino tail modified analogues (**6–17**) were synthesized utilizing the Knoevenagel condensation and a suite of commercially available *N*-alkylated indole-3-carbaldehydes possessing a range functionalities including hydroxyls, amides, morpholines, and aromatic moieties (Scheme 2).<sup>34–41</sup>

### Scheme 2<sup>a</sup>

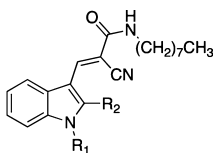


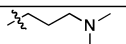
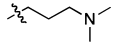
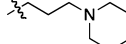
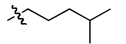
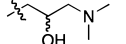
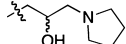
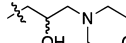
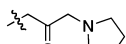
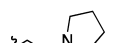
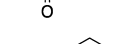
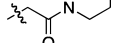
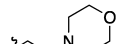
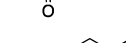
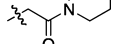
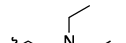
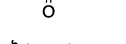
for details of R<sub>1</sub> and R<sub>2</sub>, see Table 1

<sup>a</sup>Reagents and conditions; (i) EtOH, microwave, 120 °C, 150 W, 20 min.

These compounds were evaluated as potential dynI inhibitors, and the outcomes of this screening are presented in Table 1. The absolute requirement of the dimethylamino tail was confirmed. Increased steric shielding of the amino nitrogen reduced activity (**4**, IC<sub>50</sub> 172 μM), while bioisosteric replacement (–N(CH<sub>3</sub>)<sub>2</sub> to –CH(CH<sub>3</sub>)<sub>2</sub>) (**5**) afforded an analogue devoid of dynI inhibition. Similarly, all amide substituted (**9–14**) and aromatic moieties (**15–17**) were inactive. The hydroxy substituted analogues (**6–8**) all displayed good to modest levels of dynamin inhibition, with IC<sub>50</sub> values in the range 4–18 μM. Interestingly here, encapsulation of the dimethylamino tail as a cyclopentyl amine had no effect on activity (**6** and **7** are equipotent with IC<sub>50</sub> values of 4.8 ± 0.6 and 4.4 ± 0.5 μM, respectively). While the –OH moiety does introduce a chiral center, we note that oxidation to the amide

Table 1. Inhibition of Purified Sheep Brain dynI GTPase Activity by Indole Analogues 1, 2, and 4–17



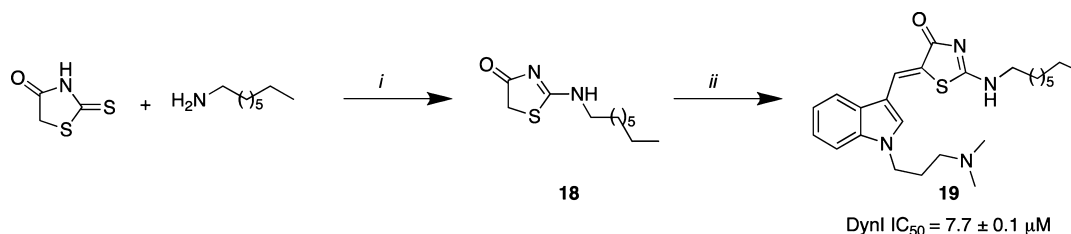
Compound	R <sub>1</sub>	R <sub>2</sub>	IC <sub>50</sub> μM <sup>[a]</sup>
1		CH <sub>3</sub>	3.3 ± 0.3
2		H	1.3 ± 0.3
4		H	172
5		CH <sub>3</sub>	Not Active
6		H	4.8 ± 0.6
7		H	4.4 ± 0.5
8		H	18.0 ± 4.1
9		H	Not Active
10		H	Not Active
11		CH <sub>3</sub>	Not Active
12		CH <sub>3</sub>	Not Active
13		CH <sub>3</sub>	Not Active
14		H	>> 300
15		H	Not Active
16		H	Not Active
17		H	Not Active

<sup>a</sup>IC<sub>50</sub> determinations are the mean ±95% confidence interval (CI) of a single experiment performed in triplicate.

removes all activity, suggesting a potential hydrogen bond donor role.

Satisfied that the *N,N*-dimethylaminopropyl was a crucial and optimal component of the indole scaffold, attention turned to the cyanoamide linker (Figure 1). Research in our group suggested that the thiazol-4(*5H*)-one moiety could function as a cyanoamide bioisostere (unpublished data), and analogue **19** was synthesized via a two-step procedure (Scheme 3).

Thiazol-4(*5H*)-one isosteric replacement of the cyanoamide moiety afforded **19**, a 7.7 ± 0.1 μM potent dynI inhibitor (Table 2). This represents only a slight reduction of activity relative to the lead **2** (IC<sub>50</sub> = 1.3 ± 0.3 μM). This suggests that the cyanoamide linker was more tolerable of chemical alterations than the dimethylamino tail, and consequently we turned our attention to the development of linker-altered analogues.

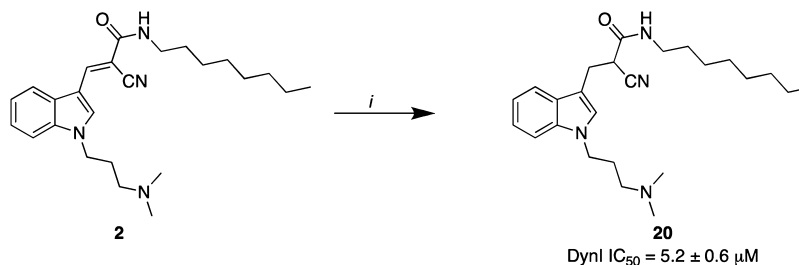
Scheme 3<sup>a</sup>

<sup>a</sup>Reagents and conditions: (i) acetonitrile, DIEA, MgCl<sub>2</sub>, rt, 48 h; (ii) 1-(3-dimethylaminopropyl)-1H-indole-3-carboxaldehyde,<sup>31</sup> EtOH, microwave, 120 °C, 150 W, 20 min.

Table 2. Inhibition of Purified Sheep Brain dynI GTPase Activity by Linker Modified Indole Analogues 19 and 20

Compound	Structure	IC <sub>50</sub> μM <sup>[a]</sup>
19		7.7 ± 0.1
20		5.2 ± 0.6

<sup>a</sup>IC<sub>50</sub> determinations are the mean ±95% confidence interval (CI) of a single experiment performed in triplicate.

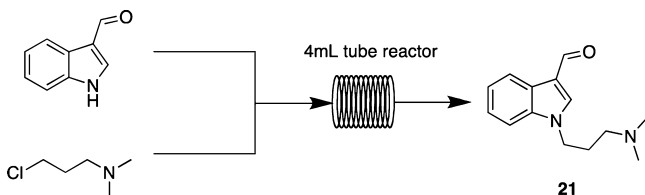
Scheme 4<sup>a</sup>

<sup>a</sup>Reagents and conditions; (i) ThalesNano H-cube hydrogenation, EtOH (conc 0.05 M), 50 °C, 50 bar, 1.0 mL/min 10% Pd/C.

Although our current synthetic methodologies had afforded numerous indole-based analogues in excellent yields and relatively short timeframes, we were eager to explore methodologies to improve synthetic efficiencies. Having access to a range of flow chemistry instrumentation, we explored its potential to optimize the synthetic approaches to these analogues, potentially leading to enhanced synthetic efficiency, increased yields, reduced reaction times and byproduct formation, potentially minimizing complications typically associated with scale-up.<sup>42–52</sup> It was envisaged that the ThalesNano H-cube (H-cube), a continuous flow hydrogenation reactor, would allow rapid access to a series of linker-altered analogues with potential modifications including saturation of the cyanoamide linker and simplification of the linker to an amine. Initially, reduction of the cyanoamide linker was investigated whereby a solution of **2** was hydrogenated at 50 °C, under 50 bar of H<sub>2</sub> pressure, with a 10% Pd/C catalyst (Scheme 4). Concentration of the eluate afforded the reduced

analogue **20** in near quantitative yields, and screening revealed it to be a 5.2 ± 0.6 μM potent dynamin inhibitor (Table 2).

Successful flow hydrogenation of **2** led us to examine the possibility of applying flow chemistry approaches to the installation of the propyl dimethylamino tail in the first step of the synthesis of this lead compound. Our previous approach relied on sodium hydride (NaH) to install the propyl dimethylamino tail onto the commercially available indole-3-carboxyaldehyde.<sup>33</sup> This suffered from unreliable yields. NaH was problematic in any proposed flow chemistry route to aldehyde **21** with the possibility of pressure build up, but of greater concern was the requirement to develop a NaH-based packed column. As flow chemistry requires all materials to be either soluble in the flow solvent or to be suitable for packing into an in-line column reactor, we thus investigated soluble bases. Using the SYRRIS FRX100 twin pump system and a 4 mL tube reactor, our initial investigations centered on the use of NaOH/MeOH mixtures (Scheme 5). As can be seen from the data presented in Table 3, even at relatively low

Scheme 5<sup>a</sup>

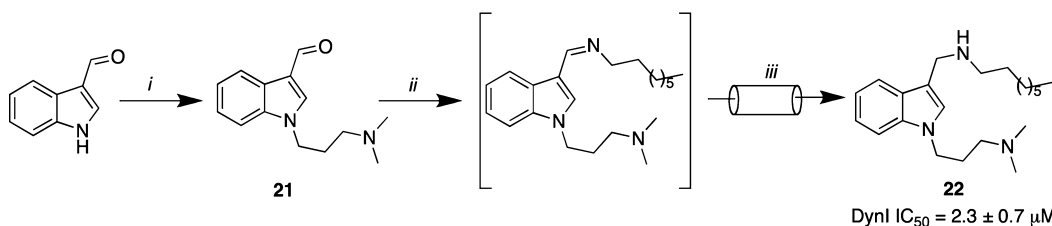
<sup>a</sup>Reagents and conditions: NaOH, 0.5 M (for solvent, see Table 3), 1 mL/min.

**Table 3. Flow Chemistry Optimization of the Addition of 3-Chloro-*N,N*-propan-1-amine with 1*H*-Indole-3-carbaldehyde<sup>a</sup>**

base	solvent	temp (°C)	yield (%)	time
NaH	THF	56	45	72 h
NaOH	MeOH	80	<20	10 min
NaOH	MeOH	90	20	10 min
NaOH	MeOH	100	23	10 min
NaOH	MeOH	110	30	10 min
NaOH	MeOH	120	35	10 min
NaOH	MeOH	130	55	10 min
NaOH	EtOH/H <sub>2</sub> O (1:1)	160	75	10 min

<sup>a</sup>Flow rate total of 1 mL/min, solutions were 0.5M in specified solvent.

temperatures of 80 °C the desired product was detectable, <20%, by <sup>1</sup>H NMR after a 10 min reaction run at a combined flow rate of 1 mL/min. Increasing the reaction temperature in 10 °C increments, under increased system pressure (FRX pressurization module), saw a steady increase in the product yield with the best conversion noted in MeOH at 130 °C of 55%. Solvent switching to EtOH/H<sub>2</sub>O (1:1) allowed the reaction to be conducted at 160 °C with a 75% conversion noted. This was a significant enhancement on our originally reported synthesis using NaH/THF for 72 h to effect a 45% yield.<sup>33</sup> Encouraged by the ease of addition under flow chemistry conditions, we re-examined our batch chemistry approaches with milder bases (than NaH). Of the numerous bases examined, cesium carbonate afforded the best outcome, with yields increased to 88%, respectively, after aqueous workup and chromatography. Thus choice of base is an important consideration with the so-called “cesium effect”.<sup>53</sup> Further optimization via the addition of potassium iodide in a Finkelstein modification gave quantitative yields of the desired product (**21**) on simple aqueous workup without the need for further purification.

Scheme 6<sup>a</sup>

<sup>a</sup>Reagents and conditions; (i) Cs<sub>2</sub>CO<sub>3</sub>, KI, ACN, reflux, 28 h; (ii) MeOH, microwave, 100 °C, 150 W, 10 min; (iii) H-cube hydrogenation, EtOH (conc 0.05 M), 50 °C, 50 bar, 1.0 mL/min 10% Pd/C.

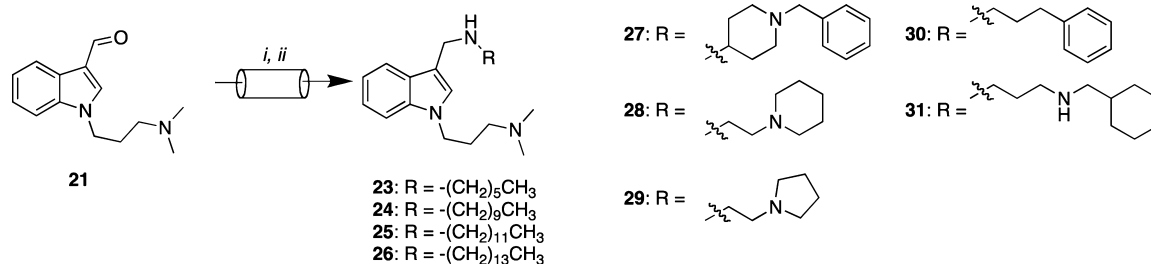
Given the success of this initial hydrogenation and our ability to replace the cyanoamide moiety with **19** and **20**, we questioned the absolute requirement for such a moiety. We investigated the potential of synthesizing additional analogues by replacing the cyanoamide with a simple amine by simple reductive amination of indole carboxaldehyde (**21**) with a series of amines in the H-cube. The imine was preformed by microwave irradiation of a suspension of octylamine, substituted indole-3-carboxaldehyde (**21**), and MgSO<sub>4</sub> in toluene for 10 min. After workup, the resultant solution was diluted and subjected to flow hydrogenation (50 °C, 50 bar H<sub>2</sub> pressure, 1 mL/min flow rate). Concentration of the eluate afforded compound **22** in a 78% yield (Scheme 6).

Both hydrogenated analogues displayed good dynI inhibitory activity with the saturated analogue **20** displaying a modest reduction in activity (IC<sub>50</sub> = 5.2 ± 0.6 μM; Table 2), while the “linker-absent” analogue **22** (IC<sub>50</sub> = 2.3 ± 0.7 μM) (Table 4),

**Table 4. Inhibition of Purified Sheep Brain dynI GTPase Activity by Analogues 22–31**

Compound	R	DynI IC <sub>50</sub> μM <sup>a</sup>
<b>22</b>	-(CH <sub>2</sub> ) <sub>7</sub> CH <sub>3</sub>	2.3 ± 0.7
<b>23</b>	-(CH <sub>2</sub> ) <sub>5</sub> CH <sub>3</sub>	9.7 ± 1.4
<b>24</b>	-(CH <sub>2</sub> ) <sub>9</sub> CH <sub>3</sub>	0.56 ± 0.09
<b>25</b>	-(CH <sub>2</sub> ) <sub>11</sub> CH <sub>3</sub>	0.76 ± 0.05
<b>26</b>	-(CH <sub>2</sub> ) <sub>13</sub> CH <sub>3</sub>	1.1 ± 0.3
<b>27</b>		9.7 ± 1.6
<b>28</b>		21.8 ± 5.1
<b>29</b>		18.6 ± 2.8
<b>30</b>		2.9 ± 0.6
<b>31</b>		2.6 ± 0.5

<sup>a</sup>IC<sub>50</sub> determinations are the mean ± 95% confidence interval (CI) of a single experiment performed in triplicate.

Scheme 7<sup>a</sup>

<sup>a</sup>Conditions and reagents; (i) MeOH, microwave, 100 °C, 150 W, 10 min; (ii) H-cube hydrogenation, EtOH (conc 0.05 M), 50 °C, 50 bar, 1.0 mL/min 10% Pd/C.

was near equipotent to the lead indole **2** ( $IC_{50} = 1.30 \pm 0.3 \mu M$ ). Thus, utilizing microwave and flow hydrogenation methodologies, the potent dynamin inhibitor **22** was prepared in an excellent yield in a simple two-step synthesis. The flow rates and concentration used correspond to a conversion of ~100 mg of compound per hour. Subsequently, we found that the initial microwave step in toluene/ $MgSO_4$  was not necessary and simple irradiation and dilution in MeOH under the same flow conditions afforded the desired compound in quantitative yields. This is highly adaptable to large-scale synthesis being only limited by the volume of reagent (at 0.05 M) and the lifespan of the catalyst cartridge.

Buoyed by this result, we set about synthesizing an additional library of compounds utilizing the microwave-hydrogenation sequential protocol. Previously significant alterations in dynamin inhibitory activity were observed with extensions and contractions of the aliphatic tail, thus a small series of analogues (**23–31**) were prepared to investigate optimum chain length (Scheme 7).

As observed with the first-generation indole-based analogues extension of the aliphatic chain significantly altered dynamin inhibitory activity (Table 4), with the hexyl (**23**) and octyl (**22**) analogues possessing  $IC_{50}$  values of 9.7 and 2.3  $\mu M$ , respectively, while the decyl analogue (**24**) displayed an  $IC_{50}$  value of 0.56  $\mu M$ , the first submicromolar potent indole-based analogue. In the first-generation indole series, significant potency drop off was noted on extending the alkyl chain from octyl (1  $IC_{50} = 3.30 \pm 0.3 \mu M$ ) to decyl ( $IC_{50} = 10.1 \mu M$ ) to dodecyl ( $IC_{50} = 32 \pm 2 \mu M$ ).<sup>31</sup> Herein, our second-generation indole analogues readily accommodate longer alkyl chains, viz decyl (**24**,  $IC_{50} = 0.56 \pm 0.09 \mu M$ ), dodecyl (**25**,  $IC_{50} = 0.76 \pm 0.05 \mu M$ ), and tetradecyl (**26**,  $IC_{50} = 1.1 \pm 0.3 \mu M$ ). We attribute this increased alkyl chain length tolerance to the removal of the  $-C=C(CN)-(CO)-$  linker moiety. The obvious penalty is an increase cLogP from 4.72 (**2**) to 5.45 (**24**) (Table 5). These analogues have incorporated relatively simple and non “drug-like” straight chain aliphatic moieties. To rectify this, a number of more “drug-like” amines were investigated as potential tail units (**27–31**). The changes were reasonably tolerated, with the chains terminating in aromatic or bulky hydrophobic units (compounds **27**, **30**, and **31**, respectively), retaining activity with the latter two being more potent (Table 4). Additionally, this small series of compounds suggest that a number of heteroatoms including cyclic groups may be incorporated within this region of the indole scaffold. This may allow fine-tuning to generate preferred physicochemical properties in the future.

Alkyl chain elongation in analogues such as **24** and **25** would be expected to promote additional off-target concerns,

**Table 5. Clathrin-Mediated Endocytosis of Tfn Inhibition in U2OS Cells by Second-Generation Indole-Based Dynamin Inhibitors**

compd	dynI $IC_{50}$ ( $\mu M$ ) <sup>a</sup>	CME $IC_{50}$ ( $\mu M$ )	cLogP <sup>b</sup>
<b>2</b>	$1.30 \pm 0.30$	$5.0 \pm 0.9^c$	$3.72^{d1}$
<b>6</b>	$4.8 \pm 0.6$	$3.5 \pm 0.5^c$	$2.71^{d1}$
<b>7</b>	$4.4 \pm 0.5$	$4.5 \pm 1.1^c$	$3.52^{d1}$
<b>22</b>	$2.3 \pm 0.7$	$3.5 \pm 0.4^c$	4.53
<b>24</b>	$0.56 \pm 0.09$	$1.9 \pm 0.3^c$	5.45
<b>25</b>	$0.76 \pm 0.05$	2.8	6.39
<b>26</b>	$1.1 \pm 0.3$	$6.8 \pm 2.0^c$	7.31
<b>15</b>	not active	not active	$5.22^{d1}$

<sup>a</sup> $IC_{50}$  determinations are the mean  $\pm 95\%$  confidence interval (CI) of a single experiment performed in triplicate. <sup>b</sup>Calculated using the OSIRIS online molecular property calculator. <sup>c</sup> $IC_{50}$  represents mean  $\pm$  SEM of pooled data from at least two independent experiments. <sup>d</sup>The OSIRIS molecular property calculator does not deal with cyanamide moieties well, these values should be used with caution.

especially possibly via accumulation in cell membranes or other off-target effects. Such interactions would not preclude the development of these compounds as therapeutic agents with other membrane interacting compounds in current clinical use.<sup>56</sup> To ascertain that this second generation of indole-based dynamin inhibitors remained relatively nontoxic to cells, a comparison was completed involving our two new most potent analogues (**24** and **25**) and our lead **2** (Figure 2). Using a Trypan Blue exclusion assay **24** and **25**, at 30  $\mu M$  drug concentration, displayed considerably less toxicity (10%) than our first-generation analogues (**2**, 80%).

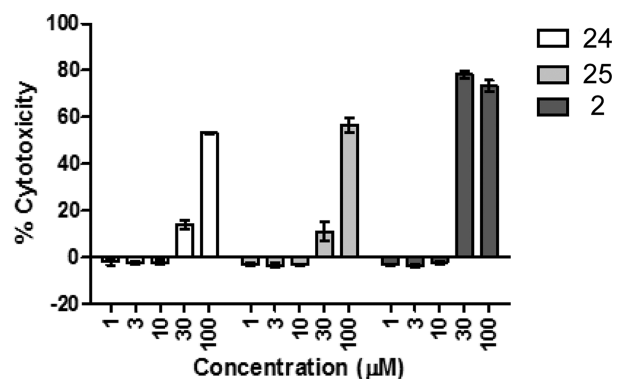


**Figure 2.** Cytotoxicity (%) of **2** and the second-generation indole analogues **24** and **25** in HeLa cells after 8 h treatment with the data normalized to drug/media background.

A subset of the most dynamin GTPase-active compounds were next selected to undergo in-cell testing for activity in clathrin mediated endocytosis (CME). This is a whole-cell assay wherein endocytosis is mediated by dynII. Six dynI-active compounds (**6**, **7**, **22**, and **24–26**) and one dynI inactive compound (**15**) were tested. Five of the six dynI active compounds were found to be potent inhibitors of CME and more potent than **2**, and the sixth analogue (**26**) was marginally less potent with an  $IC_{50}$  of  $6.8 \pm 2.0 \mu M$ . The most potent, **24**, with a CME  $IC_{50} = 1.9 \mu M$ , was 3-fold more active than **2** (Table 5); the remaining CME active analogues returned CME  $IC_{50}$  values of 2.8–6.8  $\mu M$ . Analogues **6** and **7**, which contain the additional –OH moiety, are essentially equipotent CME and dynI inhibitors, with CME  $IC_{50}$  values of  $3.5 \pm 0.5$  and  $4.5 \pm 1.1$  and dynI  $IC_{50}$  values of  $4.8 \pm 0.6$  and  $4.4 \pm 0.5 \mu M$ , respectively. This may be due to cell permeability, with only **6** and **7** having cLogP values less than 4. This highlights the importance of including physicochemical properties in the design of the next generation dynole inhibitors. The dynamin inactive analogue **15** was also inactive in cells against CME, supporting the likelihood that there is on-target specificity (Table 5).

Given the development of **24** (which we now call the Dynole 2–24 compound), we were keen to determine if it may have any selectivity for dynI vs dynII and to compare it to our lead **2**.  $IC_{50}$  values are arbitrary numbers that primarily depend on the enzyme concentration employed in the assay because the analogues bind to the enzymes. It is therefore appropriate to compare the two dynamins under normalized GTPase assay conditions wherein the concentration of each dynamin was maintained at the same 50 nM (Table 6). This change was

**Table 6. dynI vs dynII Selectivity of 2 and 24 Using Normalized Assay Conditions<sup>a</sup>**

compd	FL-dynI $IC_{50}$ ( $\mu M$ )	FL-dynII $IC_{50}$ ( $\mu M$ )	dynI/dynII selectivity
<b>2</b>	$6.9 \pm 1.0$	$16 \pm 10$	2.3
<b>24</b>	$1.7 \pm 0.3$	$5.4 \pm 7.5$	4.4

<sup>a</sup>GTPase assays for dynamin I and II were normalized so that  $IC_{50}$  values for the two enzymes can be directly compared. The assays contained 50 nM dyn I or II (pre-incubated with 10  $\mu g/mL$  PS for 15 min at RT), 300  $\mu M$  GTP, 1  $\mu g/mL$  leupeptin, and 0.1  $\mu M$  AEBSF. The reaction time for dynI and II assays were 10 and 90 min, respectively.

made because the PS-stimulated activity of dynII was considerably lower than that of dynI, in part due to its very high intrinsic basal activity,<sup>54</sup> thus its GTPase activity was not within the linear part of the Malachite Green assay unless elevated enzyme concentrations were used. In the normalized assay, all other assay conditions were the same except for the reaction time. Therefore the  $IC_{50}$  values for dynI under these normalized conditions (Table 6, 50 nM) are higher than those observed in Table 4 (at 20 nM dynI). This revealed that **2** is 2-fold dynI-selective, while **24** is 4.4-fold dynI-selective (Table 6).

## CONCLUSION

Our work represents a significant enhancement on the dynamin inhibition SAR of the indole-based dynamin inhibitor scaffold and highlights a number of advancements in the path to drug development for these compounds. SAR showed that encapsulation of the *N,N*-dimethylaminopropyl moiety was permitted if a  $\beta$ -hydroxy substituent was added, with terminal

pyrrolidine, piperidine, and morpholine moieties retaining activity. In the absence of the  $\beta$ -hydroxy substituent, encapsulation of the *N,N*-dimethylaminopropyl moiety was not tolerated and was a crucial and optimal component for activity. The overall SAR of the cyanoamide moiety identified three isosteric modifications that either retained or enhanced activity: reduction to a  $\beta$ -methylamino amide or replacement with a thiazole-4(*5H*)-one or a secondary amine. Significant enhancements were observed with the introduction of the secondary amine. Current ongoing investigations are focused on surveying an additional suite of drug-like amines, and the results of these investigations will be reported in due course.

The flow chemistry steps of the synthesis produced important advances in the rapid optimization of the reaction conditions, a significant yield enhancement, and the use of more environmentally friendly reagents relative to the original synthesis that required NaH/THF. The combination of microwave and flow chemistry methodologies allowed the identification of batch reaction conditions, yielding significant quantities of these second-generation dynamin inhibitors to be generated in high yields and with minimum reaction workup. In particular, the Finkelstein modification using KI/CaCO<sub>3</sub> afforded virtually quantitative yields of the *N*-alkylated products. Therefore our work represents the development of a vastly simplified route to these compounds.

The decyl amine analogue **24** (dynI  $IC_{50} = 0.56 \pm 0.09 \mu M$ ) is the first indole to elicit submicromolar activity against dynamin GTPase activity and only the second class of dynamin inhibitor to be submicromolar potent. A range of these second-generation indole analogues exhibited potent in-cell inhibition of CME, indicating that they retain on-target specificity. Despite that our inclusion of straight alkyl chains has the potential to promote membrane interactions off-target activity, **24** has a reduced toxicity profile. Indole **24** also displays enhanced dynII inhibition as well as a small improvement in dynI vs dynII selectivity relative to **2**. The enhanced dynII inhibition correlates with enhanced CME block in U2OS cells, and this compound is therefore the most potent reported *in-cell* inhibitor of dynamin mediated CME.

## EXPERIMENTAL SECTION

**Biology. Materials.** Phosphatidylserine (PS) and Tween 80 were from Sigma-Aldrich (St Louis, CA). 4-(2-Aminoethyl)-benzenesulfonyl fluoride hydrochloride (AEBSF) was from Calbiochem (USA). GTP was from Roche Applied Science (Germany), and leupeptin was from Bachem (Bubendorf, Switzerland). Gel electrophoresis reagents, equipment, and protein molecular weight markers were from Bio-Rad (Hercules, CA). Paraformaldehyde (PFA) was from Merck Pty Ltd. (Kilsyth, Australia). Phosphate buffered salts, fetal bovine serum (FBS), and Dulbecco's Minimal Essential Medium (DMEM) were from Invitrogen (Mount Waverley, Victoria, Australia). Alexa-594 conjugated Tfn (Tfn-A594) and DAPI were from Molecular Probes (Oregon, USA). All other reagents were of analytical reagent grade or better.

**Drugs.** Drugs were made in-house. They were made up as stock solutions (30 mM) in 100% DMSO and diluted in 50% v/v DMSO/20 mM Tris/HCl pH 7.4 or cell media prior to further dilution in the assay. The final DMSO concentration in the GTPase or endocytosis assays was at most 3% or 1%, respectively. The GTPase assay for dynI was unaffected by DMSO up to 3.3%. Drug stocks can be stored at  $-20 \text{ }^{\circ}\text{C}$  for several months.

**Protein Production.** Endogenous dynI (18 mg) was purified from a sheep brain by extraction from the peripheral membrane fraction of whole brain and affinity purification on GST-Amph2-SH3-sepharose as described.<sup>23</sup> Full length rat dynII (His-6-tagged) was

expressed as a recombinant protein from a pIEx-6 vector in insect cells (SF21) using polyethylenimine as the transfection reagent using a DNA: polyethylenimine = 1:5 for 48 h and was purified by affinity purification on GST–Amph2–SH3–sepharose as described previously.<sup>29</sup>

**Malachite Green GTPase Assay: Standard Assay Conditions (dynI).** Malachite Green method was used for the sensitive colorimetric detection of orthophosphate ( $P_i$ ). The assay is based on stimulation of native sheep brain-purified dynI by sonicated PS liposomes.<sup>55</sup> Although in our earlier studies we used 200 nM dynI, in the present study we used 20 nM, requiring an optimization of assay volumes and the Malachite Green reagent.<sup>24,26</sup> Purified dynI (20 nM) (diluted in 6 mM Tris/HCl, 20 mM NaCl, 0.01% Tween 80, pH 7.4) was incubated in GTPase assay buffer (5 mM Tris/HCl, 10 mM NaCl, 2 mM  $Mg^{2+}$ , 0.05% Tween 80, pH 7.4, 1  $\mu$ g/mL leupeptin, and 0.1 mM AEBF) and GTP 0.3 mM in the presence of test compound for 30 min at 37 °C. The final assay volume was 150  $\mu$ L in round-bottomed 96-well plates. Plate incubations were performed in a dry heating block with shaking at 300 rpm (Eppendorf Thermomixer). Dynamine I GTPase activity was maximally stimulated by addition of different concentrations of phosphatidylserine liposomes. This assay can also be conducted in the absence of Tween with little effect on the  $IC_{50}$  values noted for the indoles listed in Tables 1, 2, and 4. The reaction was terminated with 10  $\mu$ L of 0.5 M EDTA pH 8.0, and the samples were stable for several hours at room temperature. To each well was added 40  $\mu$ L of Malachite Green solution (2% w/v ammonium molybdate tetrahydrate, 0.15% w/v malachite green, and 4 M HCl; the solution was passed through 0.45  $\mu$ m filters and stored in the dark for up to 2 months at room temperature). Color developed for 5 min (and was stable up to 2 h), and the absorbance was determined on a microplate spectrophotometer at 650 nm. Phosphate release was quantified against a standard curve of sodium dihydrogen orthophosphate monohydrate (baked dry at 110 °C overnight) which was run in each experiment. GraphPad Prism 5 (GraphPad Software Inc., San Diego, CA) was used for plotting data points and analysis of enzyme kinetics using nonlinear regression.

**Malachite Green GTPase Assay: Normalized Assay Conditions (dynI and II).** Normalized assay conditions were developed in order to compare the  $IC_{50}$  values for dynamine I and II at the same enzyme concentration: 50 nM dynI and II (diluted in 6 mM Tris/HCl, 20 mM NaCl, 0.01% Tween 80, pH 7.4) were used, with 10  $\mu$ g/mL PS being used to stimulate both. DynI or II were preincubated with PS for 15 min at room temperature without shaking (in 6 mM Tris-HCl, 20 mM NaCl, 0.01% Tween-80, pH 7.4), following which the mixture was incubated in GTPase assay buffer (5 mM Tris-HCl, 10 mM NaCl, 2 mM  $Mg^{2+}$ , 0.05% Tween-80, pH 7.4, 1  $\mu$ g/mL leupeptin, and 0.1 mM AEBF) with 300  $\mu$ M GTP in the presence of test compound at 37 °C with constant shaking at 800 rpm. The reaction times were 10 and 90 min for dynI and II, respectively, in order to maintain activity within the dynamic range of the assay. Final assay volume and the shaking conditions were the same for both assays. The reactions were terminated with 10  $\mu$ L of 0.5 M EDTA, pH 8.0.

**Texas Red-Tfn Uptake.** U2OS cells were cultured in DMEM supplemented with 10% FBS at 37 °C and in 5%  $CO_2$  in a humidified incubator. Tfn uptake was analyzed based on methods previously described.<sup>33</sup> Briefly, cells were grown in fibronectin-coated (5  $\mu$ g/mL) 96-well glass-bottomed plates. The cells were serum-starved overnight (16 h) in DMEM minus FBS. Cells were then incubated with test compounds (1–300  $\mu$ M) or vehicle for 30 min prior to addition of 4  $\mu$ g/mL Tfn-TxR for 8 min at 37 °C. Cell surface-bound Tfn was removed by incubating the cells in an ice-cold acid wash solution (0.2 M acetic acid + 0.5 M NaCl, pH 2.8) for 10 min and washed with ice cold PBS for 5 min. Cells were immediately fixed with 4% PFA for 10 min at 37 °C. Nuclei were stained using DAPI. Quantitative analysis of the inhibition of Tfn-TxR endocytosis in U2OS cells was performed on large numbers of cells by an automated acquisition and analysis system (Image Xpress Micro, Molecular Devices, Sunnyvale, CA). Nine images were collected from each well, averaging 40–50 cells per image. The average integrated intensity of Tfn-TxR signal per cell was calculated for each well using IXM system, and the data expressed as a

percentage of control cells (vehicle treated). The average number of cells for each data point was ~1200.  $IC_{50}$  values were calculated using Graphpad Prism v5, and data was expressed as mean  $\pm$  95% confidence interval (CI) for three wells and ~1200 cells.

**Cell Viability Assay.** Cell viability and membrane integrity was assessed by the Trypan Blue exclusion assay. Cells were seeded into a 10 cm dish at a density of  $1 \times 10^5$  cells per dish. On day 0 (24 h after seeding), cells were treated in the presence and absence of compounds or vehicle control (0.5% DMSO) for 7 days. Cells (floating and adherent) were collected, and cell viability was measured by Vi-CELL XR cell viability analyzer 2.03 (Beckman Coulter).

**Chemistry. General Methods.** All reagents were purchased from Sigma-Aldrich, Matrix Scientific, or Lancaster Synthesis and were used without purification. With the exception of THF (anhydrous >99%) obtained from Sigma-Aldrich, all solvents were redistilled from glass prior to use.

$^1H$  and  $^{13}C$  NMR spectra were recorded on a Bruker Avance AMX 300 MHz spectrometer at 300.1315 and 75.4762 MHz, respectively. Chemical shifts ( $\delta$ ) are reported in parts per million (ppm) measured relative to the internal standards, and coupling constants ( $J$ ) are expressed in hertz (Hz). Mass spectra were recorded on a Shimadzu LCMS 2010 EV using a mobile phase of 1:1 acetonitrile:H<sub>2</sub>O with 0.1% formic acid.

Melting points were recorded on a Stuart Scientific melting point apparatus (UK) and are uncorrected. Thin layer chromatography (TLC) was performed on Merck silica gel 60 F<sub>254</sub> precoated aluminum plates with a thickness of 0.2 mm. Column chromatography was performed under “flash” conditions on Merck silica gel 60 (230–400 mesh) or using the Biotage SP4 flash purification system with a 100 g prepacked snap column.

All compounds were >95% pure as determined by combustion analysis.

A CEM Discover BenchMate microwave (120 °C, 200 W, 1 h) was used to perform several refluxes. Hydrogenations were performed using the ThalesNano H-cube continuous-flow hydrogenation reactor utilizing a palladium–carbon (CatCart) catalyst, a flow rate of 1 mL/min, 40 bar of pressure, and column temperature 40 °C. Optimization of the addition to indole-3-carboxaldehyde were conducted using the SYRRIS FRX100 equipped with a 4 mL tube reactor and a FRX pressurization module.

**General Procedure 1. 1-(3-Piperidin-1-yl-propyl)-1H-indole-3-carbaldehyde (5).** To a stirred solution of indole-3-carbaldehyde (0.99 g, 6.8 mmol) and anhydrous THF (30 mL) at 0 °C was added sodium hydride (50% dispersion in oil, 2.0 g) in small portions over a 10 min period. The resulting pink solution was stirred at 0 °C for 30 min prior to the addition of 1-(3-chloropropyl)piperidine monohydrochloride (1.44 g, 7.3 mmol). The reaction mixture was heated at reflux for 72 h, quenched with water (50 mL), the organic material extracted with EtOAc (3  $\times$  40 mL), dried ( $MgSO_4$ ), and concentrated in vacuo. The resulting brown solid was purified by flash chromatography (1:1 MeOH/DCM) to afford 1-(3-piperidin-1-yl-propyl)-1H-indole-3-carbaldehyde (0.12 g, 7%) as an orange oil.  $^1H$  NMR ( $CDCl_3$ ):  $\delta$  10.00 (1H, s), 8.31 (1H, m), 7.81 (1H, s), 7.42 (1H, m), 7.35 (2H, m), 4.31 (2H, t,  $J$  = 6.6 Hz), 2.45 (4H, m), 2.34 (2H, t,  $J$  = 6.9 Hz), 2.17 (2H, quin,  $J$  = 6.9 Hz), 1.68 (4H, m), 1.49 (2H, m).  $^{13}C$  NMR ( $CDCl_3$ ):  $\delta$  184.0, 138.2, 136.8, 125.7, 124.1, 123.4, 122.4, 121.6, 109.5, 54.5, 53.8, 44.2, 25.7, 24.9, 23.5. MS (ES+):  $m/z$  271 (M + 1, 100%).

**2-Methyl-1-(4-methylpentyl)-1H-indole-3-carbaldehyde (4).** Compound 2 was synthesized using general procedure 1, 2-methyl-1H-indole-3-carbaldehyde (3.0 g, 18.9 mmol), 5-chloro-2-methylpentane (3.1 g, 18.9 mmol), sodium hydride (50% dispersion in oil, 2.0 g), and THF (20 mL) to afford the title compound as a yellow oil (2.67 g, 58%).  $^1H$  NMR ( $CDCl_3$ ):  $\delta$  10.12 (1 H, s), 8.28 (1 H, td,  $J$  = 5.7, 2.4 Hz), 7.35–7.19 (3 H, m), 4.00 (2 H, t,  $J$  = 6.7 Hz), 2.61 (3 H, s), 1.85–1.66 (2 H, m), 1.56 (1 H, sep,  $J$  = 6.6 Hz) 1.24 (2 H, m), 0.89 (6 H, d,  $J$  = 6.6 Hz).  $^{13}C$  NMR ( $CDCl_3$ ):  $\delta$  183.6, 146.7, 135.7, 125.3, 122.4, 122.1, 120.3, 113.6, 109.0, 43.1, 35.4, 27.2, 26.9, 21.9, 9.9. MS (ES+):  $m/z$  244 (M + 1, 100%).



**2-Cyano-*N*-octylacetamide (3).** A solution of methyl cyanoacetate (2.16 g, 21.8 mmol), *n*-octylamine (2.83 g, 21.8 mmol), and MeOH (10 mL) were stirred at room temperature for 4 h. The resulting solid was collected by vacuum filtration and recrystallized from EtOH to afford 2-cyano-*N*-octylacetamide (3.38 g, 79%) as a white flaky solid (mp 68–70 °C). <sup>1</sup>H NMR (CDCl<sub>3</sub>): δ 6.48 (1H, bs), 3.37 (2H, s), 3.25 (2H, q, *J* = 6.6 Hz), 1.51 (2H, quin, *J* = 6.6 Hz), 1.28 (10H, m), 0.86 (3H, t, *J* = 6.3 Hz). <sup>13</sup>C NMR (CDCl<sub>3</sub>): δ 160.6, 114.4, 39.8, 31.2, 28.9, 28.6, 28.5, 26.2, 25.3, 22.0, 13.9. MS (ES<sup>+</sup>): *m/z* 197 (*M* + 1, 100%).

**General Procedure 2.** **3-(1-(3-Piperidin-1-yl-propyl)-1*H*-indol-3-yl)-2-cyano-*N*-octylacrylamide (4).** A solution of 1-(3-piperidin-1-ylpropyl)-1*H*-indole-3-carbaldehyde (0.09 g, 0.33 mmol), 2-cyano-*N*-octylacetamide (0.07 g, 0.36 mmol), piperidine (0.1 mL), and EtOH (5 mL) was irradiated with microwaves (120 °C, 150 W) for 20 min. The reaction vessel was cooled and placed on ice, and the resulting precipitate was recrystallized from ethanol to afford 3-(1-(3-piperidin-1-yl-propyl)-1*H*-indol-3-yl)-2-cyano-*N*-octylacrylamide (46 mg, 31%) as a yellow crystalline solid (mp 116–117 °C). <sup>1</sup>H NMR (DMSO-*d*<sub>6</sub>): δ 8.45 (1H, s), 8.40 (1H, s), 8.23 (1H, t, *J* = 5.7 Hz), 7.93 (1H, d, *J* = 7.2 Hz), 7.66 (1H, d, *J* = 7.8 Hz), 7.30 (2H, m), 4.38 (2H, t, *J* = 6.6 Hz), 3.20 (2H, q, *J* = 6.4 Hz), 2.24 (4H, m), 2.13 (2H, t, *J* = 6.3 Hz), 1.93 (2H, quin, *J* = 6.3 Hz), 1.49 (6H, m), 1.36 (2H, m), 1.27 (10H, m), 0.86 (3H, t, *J* = 6.4 Hz). <sup>13</sup>C NMR (DMSO-*d*<sub>6</sub>): δ 161.8, 141.1, 135.9, 132.8, 127.7, 123.2, 121.6, 118.5, 118.5, 111.1, 108.6, 97.4, 54.7, 53.8, 44.4, 39.8, 31.1, 28.9, 28.6, 28.5, 26.3, 26.1, 25.4, 24.0, 22.0, 13.8. MS (ES<sup>+</sup>): *m/z* 449 (*M* + 1, 100%).

**2-Cyano-3-(2-methyl-1-(4-methylpentyl)-1*H*-indol-3-yl)-*N*-octylacrylamide (5).** Compound 5 was synthesized using general procedure 2, 2-methyl-1-(4-methylpentyl)-1*H*-indole-3-carbaldehyde (2.30 g, 9.46 mmol), 2-cyano-*N*-octylacetamide (0.45 g, 2.30 mmol), piperidine (0.1 mL), and EtOH (5 mL). Recrystallization from EtOH afforded the title compound as a yellow solid (2.47 g, 62%), mp 96–98 °C. <sup>1</sup>H NMR (CDCl<sub>3</sub>): δ 8.59 (1H, s), 8.19–8.12 (1H, m), 7.34–7.23 (3H, m), 6.37 (1H, t, *J* = 5.5 Hz), 4.07 (2H, t, *J* = 7.6 Hz), 3.47 (2H, q, *J* = 7.6 Hz), 3.46–3.38 (1H, m), 2.56 (3H, s), 1.86–1.70 (2H, m), 1.68–1.57 (2H, m), 1.68–1.50 (2H, m), 1.46–1.24 (8H, m), 1.20 (2H, t, *J* = 7.6 Hz), 0.89 (9H, dd, *J* = 6.7, 3.3 Hz). <sup>13</sup>C NMR (CDCl<sub>3</sub>): δ 161.9, 145.5, 144.2, 136.6, 124.9, 122.4, 121.4, 121.2, 119.0, 109.2, 108.7, 96.043.7, 39.9, 35.4, 31.2, 29.0, 28.7, 28.6, 27.2, 26.9, 26.4, 22.0, 21.8, 13.5, 11.3. MS (ES<sup>+</sup>): *m/z* 422 (*M* + 1, 100%).

**3-(1-(3-Dimethylamino-2-hydroxy-propyl)-1*H*-indol-3-yl)-2-cyano-*N*-octylacrylamide (6).** Compound 6 was synthesized utilizing general procedure 2, 1-(3-dimethylamino-2-hydroxy-propyl)-1*H*-indole-3-carbaldehyde (0.20 g, 0.81 mmol), and 2-cyano-*N*-octylacetamide (0.17 g, 0.89 mmol). Recrystallization from EtOH afforded 3-(1-(3-dimethylamino-2-hydroxy-propyl)-1*H*-indol-3-yl)-2-cyano-*N*-octylacrylamide (120 mg, 35%) as a yellow solid, mp 103–105 °C. <sup>1</sup>H NMR (DMSO-*d*<sub>6</sub>): δ 8.48 (1H, s), 8.40 (1H, s), 8.16 (1H, t, *J* = 5.6 Hz), 7.91 (1H, dd, *J* = 7.1 Hz, 1.3 Hz), 7.62 (1H, d, *J* = 7.6 Hz), 7.29 (2H, m), 5.02 (1H, bs), 4.46 (1H, dd, *J* = 11.1 Hz, 3.2 Hz), 4.20 (1H, dd, *J* = 7.2 Hz, 6.9 Hz), 3.94 (1H, m), 3.21 (2H, q, *J* = 6.7 Hz), 2.20 (8H, m), 1.50 (2H, quin, *J* = 6.3 Hz), 1.27 (10H, m), 0.86 (3H, t, *J* = 6.3 Hz). <sup>13</sup>C NMR (DMSO-*d*<sub>6</sub>): δ 161.8, 141.0, 136.5, 133.8, 127.5, 122.9, 121.4, 118.4, 118.2, 111.3, 108.4, 97.2, 67.1, 62.5, 50.8, 45.8, 39.8, 31.0, 28.9, 28.5, 28.4, 26.2, 21.9, 13.7. MS (ES<sup>+</sup>): *m/z* 425 (*M* + 1, 100%).

**3-(1-(2-Hydroxy-3-pyrrolidin-1-ylpropyl)-2-methyl-1*H*-indol-3-yl)-2-cyano-*N*-octylacrylamide (7).** Compound 7 was synthesized utilizing general procedure 2, 1-(2-hydroxy-3-pyrrolidin-1-ylpropyl)-2-methyl-1*H*-indole-3-carbaldehyde (0.19 g, 0.67 mmol), and 2-cyano-*N*-octylacetamide (0.15 g, 0.76 mmol). Recrystallization from EtOH afforded 3-(1-(2-hydroxy-3-pyrrolidin-1-ylpropyl)-2-methyl-1*H*-indol-3-yl)-2-cyano-*N*-octylacrylamide (110 mg, 35%) as a yellow solid, mp 129–131 °C. <sup>1</sup>H NMR (DMSO-*d*<sub>6</sub>): δ 8.33 (1H, s), 8.11, (1H, t, *J* = 5.6 Hz), 7.95 (1H, d, *J* = 7.2 Hz), 7.54 (1H, d, *J* = 7.6 Hz), 7.23 (2H, m), 5.05 (1H, d, *J* = 4.8 Hz), 4.40 (2H, dd, *J* = 14.7 Hz, 2.9 Hz), 4.15 (2H, dd, *J* = 8.4 Hz, 6.3 Hz), 3.92 (1H, m), 3.20 (2H, q, *J* = 6.6 Hz), 2.60 (4H, m), 2.52 (2H, m), 2.45 (3H, s), 1.71 (4H, m), 1.51 (2H,

quin, *J* = 6.6 Hz), 1.28 (10H, m), 0.86 (3H, t, *J* = 6.3 Hz). <sup>13</sup>C NMR (DMSO-*d*<sub>6</sub>): δ 162.2, 146.8, 144.3, 137.4, 124.4, 122.2, 121.0, 120.8, 118.4, 110.7, 107.4, 98.2, 68.2, 60.0, 54.2, 48.3, 39.8, 31.2, 29.0, 28.6, 28.5, 26.3, 23.1, 22.0, 13.9, 11.8. MS (ES<sup>+</sup>): *m/z* 465 (*M* + 1, 100%).

**3-(1-(2-Hydroxy-3-morpholinopropyl)-1*H*-indol-3-yl)-2-cyano-*N*-octylacrylamide (8).** Compound 8 was synthesized utilizing general procedure 2, 1-(2-hydroxy-3-morpholin-4-yl-propyl)-1*H*-indole-3-carbaldehyde (0.18 g, 0.63 mmol), and 2-cyano-*N*-octylacetamide (0.14 g, 0.73 mmol). Recrystallization from EtOH afforded 3-(1-(2-hydroxy-3-morpholinopropyl)-1*H*-indol-3-yl)-2-cyano-*N*-octylacrylamide (270 mg, 92%) as an orange oil. <sup>1</sup>H NMR (CDCl<sub>3</sub>): δ 8.66 (1H, s), 8.46 (1H, s), 7.87 (1H, dd, *J* = 6.9 Hz, 1.8 Hz), 7.47 (dd, *J* = 6.9 Hz, 1.8 Hz), 7.34 (2H, m), 4.34 (1H, dd, *J* = 14.4 Hz, 3.6 Hz), 4.23 (1H, dd, *J* = 14.3 Hz, 6.0 Hz), 4.14 (1H, m), 3.70 (4H, m), 3.45 (2H, q, *J* = 6.6 Hz), 2.65 (2H, m), 2.40 (4H, m), 1.61 (2H, quin, *J* = 6.9 Hz), 1.35 (10H, m), 0.89 (3H, t, *J* = 6.9 Hz). <sup>13</sup>C NMR (CDCl<sub>3</sub>): δ 161.7, 143.9, 136.8, 133.4, 128.3, 123.7, 122.4, 119.4, 118.9, 110.6, 110.4, 95.9, 66.9, 65.7, 61.4, 53.6, 50.7, 40.4, 31.8, 29.6, 29.3, 29.2, 26.9, 22.6, 14.1. MS (ES<sup>+</sup>): *m/z* 467 (*M* + 1, 100%).

**3-(1-(2-Cyclopentylamino-2-oxoethyl)-1*H*-indol-3-yl)-2-cyano-*N*-octylacrylamide (9).** Compound 9 was synthesized utilizing general procedure 2, *N*-cyclopentyl-2-(3-formylindol-1-yl)acetamide (0.20 g, 0.75 mmol), and 2-cyano-*N*-octylacetamide (0.16 g, 0.79 mmol). Recrystallization from EtOH afforded 3-(1-(2-cyclopentylamino-2-oxoethyl)-1*H*-indol-3-yl)-2-cyano-*N*-octylacrylamide (157 mg, 47%) as a yellow solid, mp 184–186 °C. <sup>1</sup>H NMR (DMSO-*d*<sub>6</sub>): δ 8.44 (2H, bs), 8.40 (1H, s), 8.26 (1H, t, *J* = 5.7 Hz), 7.93 (1H, dd, *J* = 7.6 Hz, 1.5 Hz), 7.48 (1H, dd, *J* = 7.5 Hz, 1.5 Hz), 7.30 (2H, m), 5.00 (2H, s), 4.00 (1H, m, *J* = 6.8 Hz), 3.21 (2H, q, *J* = 6.5 Hz), 1.81 (2H, m), 1.67 (2H, m), 1.51 (4H, m), 1.42 (2H, m), 1.28 (10H, m), 0.86 (3H, t, *J* = 6.6 Hz). <sup>13</sup>C NMR (DMSO-*d*<sub>6</sub>): δ 165.6, 161.8, 141.1, 136.4, 133.8, 127.6, 123.4, 121.8, 118.5, 118.5, 110.9, 108.8, 97.8, 50.6, 49.3, 39.8, 32.3, 31.2, 29.0, 28.7, 28.6, 26.4, 23.4, 22.1, 14.0. MS (ES<sup>+</sup>): *m/z* 449 (*M* + 1, 100%).

**3-(1-(2-Oxo-2-pyrrolidin-1-yl-ethyl)-1*H*-indol-3-yl)-2-cyano-*N*-octylacrylamide (10).** Compound 10 was synthesized utilizing general procedure 2, 1-(2-oxo-2-pyrrolidin-1-yl-ethyl)-1*H*-indole-3-carbaldehyde (0.20 g, 0.77 mmol), and 2-cyano-*N*-octylacetamide (0.16 g, 0.84 mmol). Recrystallization from EtOH afforded 3-(1-(2-oxo-2-pyrrolidin-1-yl-ethyl)-1*H*-indol-3-yl)-2-cyano-*N*-octylacrylamide (278 mg, 83%) as a yellow crystalline solid, mp 144–145 °C. <sup>1</sup>H NMR (DMSO-*d*<sub>6</sub>): δ 8.41 (1H, s), 8.40 (1H, s), 8.26 (1H, t, *J* = 5.4 Hz), 7.92 (1H, dd, *J* = 6.9 Hz, 2.4 Hz), 7.55 (1H, d, *J* = 8.6 Hz), 7.28 (2H, m), 5.32 (2H, s), 3.61 (2H, t, *J* = 6.7 Hz), 3.30 (2H, t, *J* = 6.7 Hz), 3.21 (2H, q, *J* = 6.5 Hz), 1.96 (2H, m), 1.83 (2H, m), 1.51 (2H, m), 1.28 (10H, m), 0.85 (3H, t, *J* = 6.6 Hz). <sup>13</sup>C NMR (DMSO-*d*<sub>6</sub>): δ 164.5, 161.8, 141.0, 136.9, 133.8, 127.4, 123.0, 121.5, 118.4, 118.2, 111.3, 108.9, 97.7, 48.5, 45.7, 44.9, 39.8, 31.1, 28.9, 28.6, 28.5, 26.3, 25.5, 23.6, 22.0, 13.8. MS (ES<sup>+</sup>): *m/z* 435 (*M* + 1, 100%).

**3-(2-Methyl-1-(2-oxo-2-piperidin-1-yl-ethyl)-1*H*-indol-3-yl)-2-cyano-*N*-octylacrylamide (11).** Compound 11 was synthesized utilizing general procedure 2, 2-methyl-1-(2-oxo-2-piperidin-1-yl-ethyl)-1*H*-indole-3-carbaldehyde (0.20 mg, 0.70 mmol), and 2-cyano-*N*-octylacetamide (0.16 g, 0.79 mmol). Recrystallization from EtOH afforded 3-(2-methyl-1-(2-oxo-2-piperidin-1-yl-ethyl)-1*H*-indol-3-yl)-2-cyano-*N*-octylacrylamide (224 mg, 69%) as a yellow solid, mp 164–166 °C. <sup>1</sup>H NMR (DMSO-*d*<sub>6</sub>): δ 8.33 (1H, s), 8.15 (1H, t, *J* = 5.7 Hz), 7.94 (1H, dd, *J* = 6.6 Hz, 2.4 Hz), 7.48 (1H, dd, *J* = 6.6 Hz, 2.4 Hz), 7.21 (2H, m), 5.30 (2H, s), 3.58 (2H, m), 3.43 (2H, m), 3.21 (2H, q, *J* = 6.6 Hz), 2.43 (3H, s), 1.65 (4H, m), 1.48 (4H, m), 1.28 (10H, m), 0.86 (3H, t, *J* = 6.6 Hz). <sup>13</sup>C NMR (DMSO-*d*<sub>6</sub>): δ 164.2, 162.2, 146.5, 144.2, 137.7, 124.4, 122.2, 120.8, 118.3, 118.2, 110.4, 107.6, 98.9, 45.2, 44.7, 42.6, 39.8, 31.2, 28.9, 28.6, 28.5, 26.3, 26.0, 25.2, 23.8, 22.0, 13.9, 11.4. MS (ES<sup>+</sup>): *m/z* 463 (*M* + 1, 100%).

**3-(2-Methyl-1-(2-morpholino-2-oxoethyl)-1*H*-indol-3-yl)-2-cyano-*N*-octylacrylamide (12).** Compound 12 was synthesized utilizing general procedure 2, 2-methyl-1-(2-morpholino-4-yl-2-oxoethyl)-1*H*-indole-3-carbaldehyde (0.2 g, 0.70 mmol), and 2-cyano-*N*-octylacetamide (0.15 g, 0.76 mmol). Recrystallization from EtOH afforded 3-(2-methyl-1-(2-morpholino-2-oxoethyl)-1*H*-indol-3-yl)-2-

ciano-*N*-octylacrylamide (140 mg, 43%) as a yellow crystalline solid, mp 156–157 °C. <sup>1</sup>H NMR (DMSO-*d*<sub>6</sub>): δ 8.34 (1H, s), 8.16 (1H, t, *J* = 5.4 Hz), 7.94 (1H, d, *J* = 7.5 Hz), 7.50 (1H, d, *J* = 7.5 Hz), 7.23 (2H, m), 5.33 (2H, s), 3.69 (4H, m), 3.61 (4H, m), 3.21 (2H, q, *J* = 6.6 Hz), 2.45 (3H, s), 1.51 (2H, quin, *J* = 5.7 Hz), 1.28 (10H, m), 0.86 (3H, t, *J* = 6.3 Hz). <sup>13</sup>C NMR (DMSO-*d*<sub>6</sub>): δ 165.0, 162.3, 146.6, 144.3, 137.8, 124.5, 122.6, 122.3, 121.0, 118.4, 110.5, 107.7, 99.1, 66.1, 46.8, 44.8, 42.0, 31.3, 29.0, 28.7, 28.6, 26.4, 22.1, 14.0, 11.6. MS (ES<sup>+</sup>): *m/z* 465 (M + 1, 100%).

3-(2-Methyl-1-(2-(4-methylpiperidin-1-yl)-2-oxoethyl)-1H-indol-3-yl)-2-cyano-*N*-octylacrylamide (**13**). Compound **13** was synthesized utilizing general procedure 2, 2-methyl-1-(2-(4-methylpiperidin-1-yl)-2-oxoethyl)-1H-indole-3-carbaldehyde (0.19 g, 0.63 mmol), and 2-cyano-*N*-octylacetamide (0.19 g, 0.97 mmol). Recrystallization from EtOH afforded 3-(2-methyl-1-(2-(4-methylpiperidin-1-yl)-2-oxoethyl)-1H-indol-3-yl)-2-cyano-*N*-octylacrylamide (188 mg, 63%) as a yellow solid, mp 171–172 °C. <sup>1</sup>H NMR (DMSO-*d*<sub>6</sub>): δ 8.33 (1H, s), 8.15 (1H, t, *J* = 5.7 Hz), 7.94 (1H, m), 7.48 (1H, m), 7.20 (2H, m), 5.31 (2H, s), 4.25 (1H, d, *J* = 12.0 Hz), 4.02 (1H, d, *J* = 12.0 Hz), 3.21 (2H, q, *J* = 6.3 Hz), 3.14 (1H, m), 2.62 (1H, m), 2.42 (3H, s), 1.75 (1H, m), 1.64 (2H, m), 1.51 (2H, quin, *J* = 6.3 Hz), 1.28 (12H, m), 0.95 (3H, d, *J* = 6.0 Hz), 0.86 (3H, t, *J* = 6.9 Hz). <sup>13</sup>C NMR (DMSO-*d*<sub>6</sub>): δ 164.2, 162.2, 146.5, 144.2, 137.7, 124.4, 122.2, 120.8, 120.8, 118.3, 110.4, 107.6, 98.9, 44.7, 44.5, 41.9, 39.8, 34.1, 33.4, 31.2, 30.2, 28.9, 28.6, 28.5, 26.3, 22.0, 21.5, 13.9, 11.5. MS (ES<sup>+</sup>): *m/z* 477 (M + 1, 100%).

3-[1-(2-Diethylamino-2-oxoethyl)-1H-indol-3-yl]-2-cyano-*N*-octylacrylamide (**14**). Compound **14** was synthesized utilizing general procedure 2, *N,N*-diethyl-2-(3-formyl-indol-1-yl)acetamide (0.20 g, 0.76 mmol), and 2-cyano-*N*-octylacetamide (0.31 g, 1.58 mmol). Recrystallization from EtOH afforded 3-[1-(2-diethylamino-2-oxoethyl)-1H-indol-3-yl]-2-cyano-*N*-octylacrylamide (152 mg, 46%) as a white solid, mp 96–97 °C. <sup>1</sup>H NMR (DMSO-*d*<sub>6</sub>): δ 8.42 (1H, s, ArH<sub>2</sub>), 8.41 (1H, s), 8.26 (1H, t, *J* = 5.4 Hz), 7.92 (1H, m), 7.44 (1H, m), 7.29 (2H, m), 5.42 (2H, s), 3.47 (2H, q, *J* = 7.0 Hz), 3.30 (2H, q, *J* = 6.6 Hz), 3.21 (2H, q, *J* = 6.6 Hz), 1.51 (2H, quin, *J* = 6.2 Hz), 1.28 (10H, m), 1.26 (3H, t, *J* = 7.2 Hz), 1.04 (3H, t, *J* = 7.2 Hz), 0.86 (3H, t, *J* = 6.1 Hz). <sup>13</sup>C NMR (DMSO-*d*<sub>6</sub>): δ 165.3, 161.8, 141.1, 136.8, 134.1, 127.5, 123.1, 121.5, 118.3, 118.2, 111.2, 108.7, 97.5, 47.7, 40.6, 40.2, 39.8, 31.2, 28.9, 28.6, 28.5, 26.3, 22.0, 14.0, 13.9, 12.9. MS (ES<sup>+</sup>): *m/z* 451 (M + 1, 100%).

3-(1-Benzyl-1H-indol-3-yl)-2-cyano-*N*-octylacrylamide (**15**). Compound **15** was synthesized utilizing general procedure 2, 1-benzylindole-3-carbaldehyde (0.46 g, 2.0 mmol), and 2-cyano-*N*-octylacetamide (0.42 g, 2.2 mmol). Recrystallization from EtOH afforded 3-(1-benzyl-1H-indol-3-yl)-2-cyano-*N*-octylacrylamide (40 mg, 50%) as a yellow crystalline solid, mp 128–130 °C. <sup>1</sup>H NMR (DMSO-*d*<sub>6</sub>): δ 8.56 (1H, s), 8.40 (1H, s), 8.24 (1H, t, *J* = 5.4 Hz), 7.92 (1H, m), 7.60 (1H, m), 7.28 (7H, m), 5.62 (2H, s), 3.33 (2H, m), 1.49 (2H, t, *J* = 6.3 Hz), 1.26 (10H, m), 0.84 (3H, t, *J* = 6.9 Hz). <sup>13</sup>C NMR (DMSO-*d*<sub>6</sub>): δ 161.7, 141.0, 136.7, 135.9, 132.6, 128.7, 127.7, 127.1, 123.4, 121.8, 118.6, 118.3, 111.5, 109.1, 98.1, 49.8, 39.8, 31.1, 28.9, 28.6, 28.5, 26.3, 22.0, 13.9. MS (ES<sup>+</sup>): *m/z* 414 (M + 1, 100%).

3-(1-Phenylsulfonyl-1H-indol-3-yl)-2-cyano-*N*-octylacrylamide (**16**). Compound **16** was synthesized utilizing general procedure 2, 1-(phenylsulfonyl)indole-3-carbaldehyde (0.48 g, 1.7 mmol), 2-cyano-*N*-octylacetamide (0.47 g, 2.4 mmol), piperidine (0.1 mL), and EtOH (5 mL). Recrystallization from EtOH afforded 3-(1-phenylsulfonyl-1H-indol-3-yl)-2-cyano-*N*-octylacrylamide (30 mg, 39%) as a white solid, mp 141–142 °C. <sup>1</sup>H NMR (DMSO-*d*<sub>6</sub>): δ 8.68 (1H, s), 8.53 (1H, t, *J* = 5.7 Hz), 8.33 (1H, s), 8.09 (2H, dd, *J* = 7.8 Hz, 1.5 Hz), 7.99 (1H, d, *J* = 8.2 Hz), 7.96 (1H, d, *J* = 8.9 Hz), 7.76 (1H, t, *J* = 7.2 Hz), 7.64 (2H, t, *J* = 7.8 Hz), 7.45 (2H, m), 3.23 (2H, q, *J* = 6.6 Hz), 1.51 (2H, quin, *J* = 6.6 Hz), 1.27 (10H, m), 0.85 (3H, t, *J* = 6.6 Hz). <sup>13</sup>C NMR (DMSO-*d*<sub>6</sub>): δ 160.5, 139.2, 136.0, 135.3, 133.4, 130.1, 128.7, 128.0, 127.0, 126.2, 124.4, 119.9, 117.0, 115.0, 113.2, 106.2, 39.8, 31.1, 28.8, 28.6, 28.5, 26.3, 22.0, 13.9. MS (ES<sup>+</sup>): *m/z* 464 (M + 1, 100%).

3-(1-(2-Benzo[d][1,3]dioxol-5-yl-amino-2-oxoethyl)-1H-indol-3-yl)-2-cyano-*N*-octylacrylamide (**17**). Compound **17** was synthesized utilizing general procedure 2, *N*-benzo[1,3]dioxol-5-yl-2-(3-formylin-

dol-1-yl)acetamide (0.20 g, 0.61 mmol), and 2-cyano-*N*-octylacetamide (0.12 g, 0.62 mmol). Recrystallization from EtOH afforded 3-(1-(2-benzo[d][1,3]dioxol-5-yl-amino-2-oxoethyl)-1H-indol-3-yl)-2-cyano-*N*-octylacrylamide (245 mg, 79%) as a yellow solid, mp 199–200 °C. <sup>1</sup>H NMR (DMSO-*d*<sub>6</sub>): δ 10.46 (1H, s), 8.51 (1H, s), 8.43 (1H, s), 8.29 (1H, t, *J* = 5.7 Hz), 7.95, (1H, dd, *J* = 7.2 Hz, 1.5 Hz), 7.57 (1H, dd, *J* = 7.2 Hz, 1.2 Hz), 7.30 (3H, m), 6.95 (1H, d, *J* = 8.4 Hz), 6.88 (1H, d, *J* = 8.4 Hz), 5.99 (2H, s), 5.28 (2H, s), 3.22 (2H, q, *J* = 6.5 Hz), 1.51 (2H, quin, *J* = 6.0 Hz), 1.28 (10H, m), 0.86 (3H, t, *J* = 6.5 Hz). <sup>13</sup>C NMR (DMSO-*d*<sub>6</sub>): δ 164.9, 161.9, 147.1, 143.2, 141.1, 136.6, 134.0, 132.9, 127.6, 123.5, 121.9, 118.5, 118.4, 112.1, 111.1, 109.0, 108.2, 101.3, 101.1, 98.1, 49.7, 39.8, 31.1, 29.1, 28.7, 28.6, 26.4, 22.1, 14.0. MS (ES<sup>+</sup>): *m/z* 501 (M + 1, 100%).

2-(Octylamino)thiazol-4(5H)-one (**18**). To a stirred solution of 2-thio-4-thiazolin-4-one (0.82 g, 6.2 mmol), 2-octylamine (1.59 g, 12.4 mmol), and acetonitrile (15 mL) was added *N,N*-diisopropylethylamine (0.72, 5.5 mmol). The mixture was cooled to 0 °C prior to the addition of MgCl<sub>2</sub> (1.70 g, 6.2 mmol). The resulting solution was stirred at room temperature for 48 h, filtered through Celite, concentrated in vacuo, dried (MgSO<sub>4</sub>), and subjected to flash silica column chromatography (1:1 hexanes:EtOAc) to afford 2-(octylamino)thiazol-4(5H)-one (0.71 g, 51%) as a yellow solid, mp 134–135 °C. <sup>1</sup>H NMR (MeOD): δ 5.74 (2 H, s), 4.34 (1 H, t, *J* = 7.1 Hz), 2.49 (2 H, qd, *J* = 17.7, 7.0 Hz), 2.16 (12 H, m), 1.76 (3 H, t, *J* = 6.6 Hz). <sup>13</sup>C NMR (MeOD): δ 188.8, 181.4, 44.5, 37.8, 31.0, 28.4, 28.3, 28.0, 25.8, 21.7, 12.5. MS (ES<sup>+</sup>): *m/z* 229 (M + 1, 100%).

5-((1-(3-(Dimethylamino)propyl)-1H-indol-3-yl)methylene)-2-(octylamino)thiazol-4(5H)-one (**19**). Compound **19** was synthesized utilizing general procedure 2, 1-(3-dimethylaminopropyl)-1H-indole-3-carbaldehyde (2.45 g, 11.0 mmol), 2-(octylamino)thiazol-4(5H)-one (**18**) (2.50 g, 11.0 mmol), piperidine (0.1 mL), and EtOH (20 mL). Recrystallization from EtOH afforded the title compound (3.13 g, 65%) as a yellow solid, mp 136–137 °C. <sup>1</sup>H NMR (DMSO-*d*<sub>6</sub>): δ 9.44 (1 H, s), 7.81 (2 H, m), 7.59 (1 H, s), 7.55 (1 H, d, *J* = 8.1 Hz), 7.25 (1 H, t, *J* = 7.3 Hz), 7.17 (1 H, t, *J* = 7.3 Hz), 4.30 (2 H, t, *J* = 6.6 Hz), 3.46 (2 H, t, *J* = 6.6 Hz), 2.15 (8 H, m), 1.96–1.81 (2 H, m), 1.56 (2 H, m), 1.21 (10 H, m), 0.82 (3 H, t, *J* = 5.7 Hz). <sup>13</sup>C NMR (DMSO-*d*<sub>6</sub>): δ 179.8, 172.0, 136.0, 130.1, 129.8, 127.2, 122.7, 120.9, 120.7, 120.3, 118.5, 110.5, 110.3, 55.3, 44.8, 44.2, 43.7, 31.1, 28.5, 28.4, 27.0, 26.2, 22.0, 13.7. MS (ES<sup>+</sup>): *m/z* 441 (M + 1, 100%).

General Procedure 3. 2-Cyano-3-(1-(3-(dimethylamino)propyl)-1H-indol-3-yl)-*N*-octylpropanamide (**20**). A solution of 2-cyano-3-(1-(3-(dimethylamino)propyl)-1H-indol-3-yl)-*N*-octylacrylamide (**2**) (0.114 g, 0.28 mmol) and EtOH (10 mL) was hydrogenated utilizing the ThalesNano H-cube system (1.0 mL/min) loaded with a 33 mm 10% Pd/C CatCart column heated to 50 °C under 50 bar of H<sub>2</sub> pressure. The eluate was concentrated in vacuo to afford 2-cyano-3-(1-(3-(dimethylamino)propyl)-1H-indol-3-yl)-*N*-octylpropanamide (0.11 g, 92%) as a yellow oil. <sup>1</sup>H NMR (CDCl<sub>3</sub>): δ 7.50 (1 H, d, *J* = 7.6 Hz), 7.30 (1 H, d, *J* = 8.1 Hz), 7.15 (1 H, t, *J* = 7.4 Hz), 7.06 (1 H, t, *J* = 7.4 Hz), 6.13 (1 H, t, *J* = 5.5 Hz), 4.12 (2 H, t, *J* = 7.2 Hz), 3.65 (2 H, td, *J* = 8.1, 6.4 Hz), 3.40 (1 H, ddd, *J* = 22.3, 14.5, 6.8 Hz), 3.22–3.05 (2 H, m), 2.43 (3 H, s), 2.26 (2 H, t, *J* = 6.9 Hz), 2.22 (6 H, s), 1.87 (2 H, p, *J* = 7.0 Hz), 1.40–1.11 (14 H, m), 0.87 (3 H, t, *J* = 6.8 Hz). <sup>13</sup>C NMR (CDCl<sub>3</sub>): δ 164.1, 135.5, 134.4, 126.6, 120.5, 118.7, 118.1, 117.2, 108.62, 104.9, 57.6, 55.96, 44.86, 40.6, 39.9, 39.7, 30.8, 28.4, 27.5, 25.8, 25.5, 21.9, 17.9, 13.5, 9.9. MS (ES<sup>+</sup>): *m/z* 215 (M + 2, 100%), 411 (M + 1, 60%).

1-(3-Dimethylaminopropyl)-1H-indole-3-carbaldehyde (**21**). To a stirred solution of indole-3-carbaldehyde (1.00 g, 6.9 mmol) in ACN (30 mL) at 0 °C was added cesium carbonate (11.2 g, 5 equiv) and potassium iodide (2.3 g, 2 equiv) in small portions. After 10 min, 3-dimethylamino-1-propyl chloride hydrochloride (2 g, 13.8 mmol, 2 equiv) was added to the resulting suspension. The reaction mixture was heated at reflux for 18 h, quenched with water (50 mL), the organic material extracted with EtOAc (3 × 40 mL), dried (MgSO<sub>4</sub>), and concentrated in vacuo to yield the desired compound as a yellow oil (1.58 g, 100%). <sup>1</sup>H NMR (CDCl<sub>3</sub>): δ 9.98 (s, 1H), 8.34–8.25 (m, 1H), 7.75 (s, 1H), 7.46–7.36 (m, 1H), 7.33–7.29 (m, 2H), 4.26 (t, *J* = 6.8 Hz, 2H), 2.21 (t, *J* = 6.7 Hz, 2H), 2.21 (s, 6H), 2.00 (t, *J* = 6.7,

6.7 Hz, 2H).  $^{13}\text{C}$  NMR ( $\text{CDCl}_3$ ):  $\delta$  184.2, 138.9, 137.0, 125.1, 123.7, 122.6, 121.8, 117.8, 110.0, 55.5, 45.1, 44.4, 27.2. MS (ES<sup>+</sup>):  $m/z$  231 ( $M + 1$ , 100%).

**General Procedure 4.** *N*-((1-(3-(Dimethylamino)propyl)-1H-indol-3-yl)methyl)octan-1-amine (**22**). A solution of 1-(3-(dimethylamino)propyl)-1H-indole-3-carbaldehyde (0.35 g, 1.52 mmol), octylamine (0.25 mL, 1.52 mmol), toluene (5.0 mL), and  $\text{MgSO}_4$  (0.5 g) was irradiated with microwaves (100 °C, 150 W) for 10 min. The resulting crude material was filtered, diluted with EtOH (30 mL, 0.05 M), and hydrogenated with the ThalesNano H-cube system (1.0 mL/min) loaded with a 33 mm 10% Pd/C CatCart column heated to 50 °C under 50 bar  $\text{H}_2$  pressure. The eluate was concentrated in vacuo to afford *N*-((1-(3-(dimethylamino)propyl)-1H-indol-3-yl)methyl) octylamine (0.43 mg, 78%) as a yellow oil.  $^1\text{H}$  NMR ( $\text{CDCl}_3$ ):  $\delta$  7.62 (1H, d,  $J = 7.8$  Hz), 7.34 (1H, d,  $J = 8.1$  Hz), 7.21 (1H, m), 7.10 (2H, m), 4.14 (2H, t,  $J = 6.9$  Hz), 3.97 (2H, s), 2.68 (2H, t,  $J = 7.2$  Hz), 2.23 (2H, t,  $J = 7.2$  Hz), 2.20 (6H, s), 1.95 (2H, quin,  $J = 6.9$  Hz), 1.53 (2H, quin,  $J = 6.9$  Hz), 1.26 (10H, m), 0.86 (3H, t,  $J = 6.9$  Hz).  $^{13}\text{C}$  NMR ( $\text{CDCl}_3$ ):  $\delta$  136.4, 127.5, 126.6, 121.5, 118.9, 118.8, 112.9, 109.5, 56.5, 49.4, 45.4, 44.4, 43.9, 31.8, 29.8, 29.5, 29.2, 28.2, 27.4, 22.6, 14.1. MS (ES<sup>+</sup>):  $m/z$  172 ( $M + 2$ , 100%), 344 ( $M + 1$ , 50%).

*N*-((1-(3-(Dimethylamino)propyl)-1H-indol-3-yl)methyl)hexan-1-amine (**23**). Compound **23** was synthesized utilizing general procedure 4, 1-(3-(dimethylamino)propyl)-1H-indole-3-carbaldehyde (**21**) (0.38 g, 1.67 mmol), and hexylamine (0.22 mL, 1.67 mmol), affording *N*-((1-(3-(dimethylamino)propyl)-1H-indol-3-yl)methyl)-hexylamine (0.49 g, 93%) as an orange oil.  $^1\text{H}$  NMR ( $\text{CDCl}_3$ ):  $\delta$  7.63 (1H, d,  $J = 7.8$  Hz), 7.34 (1H, d,  $J = 8.1$  Hz), 7.21 (1H, m), 7.10 (2H, m), 4.14 (2H, t,  $J = 6.9$  Hz), 3.98 (2H, s), 2.69 (2H, t,  $J = 7.3$  Hz), 2.24 (2H, t,  $J = 7.0$  Hz), 2.20 (6H, s), 1.95 (2H, quin,  $J = 6.9$  Hz), 1.52 (2H, quin,  $J = 7.1$  Hz), 1.30 (6H, m), 0.87 (3H, t,  $J = 6.7$  Hz).  $^{13}\text{C}$  NMR ( $\text{CDCl}_3$ ):  $\delta$  136.6, 127.7, 126.8, 121.7, 119.1, 119.0, 113.1, 109.7, 56.7, 49.6, 45.6, 44.6, 44.1, 31.9, 29.9, 28.4, 27.2, 22.8, 14.2. MS (ES<sup>+</sup>):  $m/z$  158 ( $M + 2$ , 100%), 316 ( $M + 1$ , 70%).

*N*-((1-(3-(Dimethylamino)propyl)-1H-indol-3-yl)methyl)decan-1-amine (**24**), Dynole 2–24. Compound **24**, Dynole 2–24, was synthesized utilizing general procedure 4, 1-(3-(dimethylamino)propyl)-1H-indole-3-carbaldehyde (**21**) (0.55 g, 2.30 mmol), and decylamine (0.44 g, 2.78 mmol), affording *N*-((1-(3-(dimethylamino)propyl)-1H-indol-3-yl)methyl)decylamine (0.42 mg, 46%) as a pale-yellow oil.  $^1\text{H}$  NMR ( $\text{CDCl}_3$ ):  $\delta$  7.63 (1H, d,  $J = 7.8$  Hz), 7.33 (1H, d,  $J = 8.1$  Hz), 7.18 (1H, m), 7.08 (2H, m), 4.13 (2H, t,  $J = 6.9$  Hz), 3.98 (2H, s), 2.69 (2H, t,  $J = 7.2$  Hz), 2.19 (2H, t,  $J = 6.9$  Hz), 2.06 (6H, s), 1.94 (2H, quin,  $J = 6.9$  Hz), 1.53 (2H, quin,  $J = 6.9$  Hz), 1.25 (14H, m), 0.88 (3H, t,  $J = 6.9$  Hz).  $^{13}\text{C}$  NMR ( $\text{CDCl}_3$ ):  $\delta$  136.4, 127.6, 126.4, 121.4, 118.9, 118.8, 113.2, 109.4, 56.5, 49.5, 45.3, 44.5, 43.8, 31.8, 29.8, 29.5, 29.2, 28.2, 27.3, 22.6, 14.0. MS (ES<sup>+</sup>):  $m/z$  186 ( $M + 2$ , 100%), 372 ( $M + 1$ , 50%).

*N*-((1-(3-(Dimethylamino)propyl)-1H-indol-3-yl)methyl)dodecan-1-amine (**25**). Compound **25** was synthesized utilizing general procedure 4, 1-(3-(dimethylamino)propyl)-1H-indole-3-carbaldehyde (**21**) (0.36 g, 1.56 mmol), and dodecylamine (0.29 g, 1.56 mmol), affording *N*-((1-(3-(dimethylamino)propyl)-1H-indol-3-yl)methyl)-dodecylamine (0.56 mg, 89%) as an orange oil.  $^1\text{H}$  NMR ( $\text{CDCl}_3$ ):  $\delta$  7.62 (1H, d,  $J = 7.8$  Hz), 7.34 (1H, d,  $J = 8.1$  Hz), 7.20 (1H, m), 7.10 (2H, m), 4.14 (2H, t,  $J = 6.9$  Hz), 3.97 (2H, s), 2.69 (2H, t,  $J = 7.2$  Hz), 2.23 (2H, t,  $J = 7.2$  Hz), 2.20 (6H, s), 1.95 (2H, quin,  $J = 6.9$  Hz), 1.52 (2H, quin,  $J = 6.9$  Hz), 1.24 (18H, m), 0.87 (3H, t,  $J = 6.9$  Hz).  $^{13}\text{C}$  NMR ( $\text{CDCl}_3$ ):  $\delta$  135.9, 127.0, 125.9, 121.0, 118.4, 118.3, 112.7, 109.0, 56.0, 49.0, 44.9, 44.0, 43.4, 31.4, 29.4, 29.1, 28.8, 27.7, 26.9, 22.1, 13.6. MS (ES<sup>+</sup>):  $m/z$  400 ( $M + 2$ , 100%), 200 ( $M + 1$ , 60%).

*N*-((1-(3-(Dimethylamino)propyl)-1H-indol-3-yl)methyl)tetradecylamine (**26**). Compound **26** was synthesized utilizing general procedure 4, 1-(3-(dimethylamino)propyl)-1H-indole-3-carbaldehyde (**21**) (0.39 g, 1.69 mmol), and tetradecylamine (0.36 g, 1.69 mmol), affording *N*-((1-(3-(dimethylamino)propyl)-1H-indol-3-yl)methyl)-tetradecylamine (0.54 mg, 75%).  $^1\text{H}$  NMR ( $\text{CDCl}_3$ ):  $\delta$  7.62 (1H, d,  $J = 7.8$  Hz), 7.34 (1H, d,  $J = 8.4$  Hz), 7.20 (1H, dt,  $J = 8.1$ , 1.2 Hz), 7.10 (2H, m), 4.14 (2H, t,  $J = 6.9$  Hz), 3.97 (2H, s), 2.69 (2H, t,  $J = 7.2$  Hz), 2.23 (2H, t,  $J = 7.2$  Hz), 2.20 (6H, s), 1.95 (2H, quin,  $J = 6.9$

Hz), 1.52 (2H, quin,  $J = 6.9$  Hz), 1.25 (22H, m), 0.87 (3H, t,  $J = 6.9$  Hz).  $^{13}\text{C}$  NMR ( $\text{CDCl}_3$ ): 136.4, 127.5, 126.4, 121.5, 118.9, 118.8, 113.3, 109.5, 56.5, 49.6, 45.4, 44.6, 43.9, 31.9, 29.9, 29.7, 29.3, 28.3, 27.4, 22.7, 14.1. MS (ES<sup>+</sup>):  $m/z$  214 ( $M + 2$ , 100%), 428 ( $M + 1$ , 70%).

*1-Benzyl-N*-((1-(3-(dimethylamino)propyl)-1H-indol-3-yl)methyl)piperidin-4-amine (**27**). Compound **27** was synthesized utilizing general procedure 4, 1-(3-(dimethylamino)propyl)-2-methyl-1H-indole-3-carbaldehyde (**21**) (0.73 g, 3.0 mmol), and 1-benzylpiperidin-4-amine (0.80 mL, 3.0 mmol), affording 1-benzyl-*N*-((1-(3-(dimethylamino)propyl)-2-methyl-1H-indol-3-yl)methyl)piperidin-4-amine (0.62 g, 49%) as a yellow solid, mp 62–64 °C.  $^1\text{H}$  NMR ( $\text{CDCl}_3$ ):  $\delta$  7.58 (1 H, d,  $J = 7.5$  Hz), 7.38–7.29 (4 H, m), 7.27 (1 H, dt,  $J = 6.9$ , 6.5, 4.0 Hz), 7.15 (1 H, dd,  $J = 11.0$ , 4.0 Hz), 7.13–7.06 (1 H, m), 4.14 (2 H, t,  $J = 7.3$  Hz), 3.96 (2 H, s), 3.53 (2 H, s), 2.89 (2 H, m), 2.69–2.54 (1 H, m), 2.44 (3 H, s), 2.30 (2 H, t,  $J = 6.9$  Hz), 2.24 (6 H, s), 2.08 (2 H, dt,  $J = 11.5$ , 2.2 Hz), 1.90 (4 H, m), 1.55 (4 H, m).  $^{13}\text{C}$  NMR ( $\text{CDCl}_3$ ):  $\delta$  138.2, 135.6, 133.1, 128.5, 127.6, 127.2, 126.3, 120.1, 118.4, 117.3, 109.7, 108.4, 62.6, 56.1, 54.0, 51.9, 44.9, 40.5, 40.3, 32.2, 27.7, 9.7. MS (ES<sup>+</sup>):  $m/z$  210 ( $M + 2$ , 100%), 419 ( $M + 1$ , 70%).

*N,N*-Dimethyl-3-(3-((2-(piperidin-1-yl)ethylamino)methyl)-1H-indol-1-yl)propan-1-amine (**28**). Compound **28** was synthesized utilizing general procedure 4, 1-(3-(dimethylamino)propyl)-1H-indole-3-carbaldehyde (**21**) (0.16 g, 0.70 mmol), and 1-(2-aminoethyl)piperidine (0.1 mL, 0.70 mmol), affording *N,N*-dimethyl-3-(3-(2-(piperidin-1-ylethylamino)methyl)-1H-indol-1-yl)propylamine (209 mg, 87%) as an orange oil.  $^1\text{H}$  NMR ( $\text{CDCl}_3$ ):  $\delta$  7.63 (1H, dd,  $J = 7.8$ , 0.9 Hz), 7.34 (1H, d,  $J = 8.1$  Hz), 7.20 (1H, dt,  $J = 7.2$ , 1.2 Hz), 7.10 (2H, m), 4.15 (2H, t,  $J = 6.9$  Hz), 4.00 (2H, s), 2.81 (2H, t,  $J = 6.3$  Hz), 2.48 (2H, t,  $J = 6.3$  Hz), 2.35 (4H, m), 2.24 (2H, t,  $J = 6.9$  Hz), 2.20 (6H, s), 1.96 (2H, quin,  $J = 6.9$  Hz), 1.51 (4H, m), 1.41 (2H, m).  $^{13}\text{C}$  NMR ( $\text{CDCl}_3$ ):  $\delta$  136.5, 127.5, 126.5, 121.6, 119.0, 118.8, 112.9, 109.5, 58.1, 56.5, 54.6, 45.8, 45.4, 44.5, 43.9, 28.2, 25.9, 24.4. MS (ES<sup>+</sup>):  $m/z$  172 ( $M + 2$ , 100%), 343 ( $M + 1$ , 30%).

*N,N*-Dimethyl-3-(3-((2-(pyrrolidin-1-yl)ethylamino)methyl)-1H-indol-1-yl)propan-1-amine (**29**). Compound **29** was synthesized utilizing general procedure 4, 1-(3-(dimethylamino)propyl)-1H-indole-3-carbaldehyde (**21**) (0.14 g, 0.61 mmol), and 1-(2-aminoethyl)pyrrolidine (0.08 mL, 0.63 mmol), affording *N,N*-dimethyl-3-(3-(2-(pyrrolidin-1-yl)ethylamino)methyl)-1H-indol-1-yl)propylamine (183 mg, 92%) as a yellow oil.  $^1\text{H}$  NMR ( $\text{CDCl}_3$ ):  $\delta$  7.63 (1H, dd,  $J = 7.8$ , 0.9 Hz), 7.34 (1H, d,  $J = 8.1$  Hz), 7.20 (1H, dt,  $J = 6.9$ , 1.2 Hz), 7.09 (2H, m), 4.15 (2H, t,  $J = 6.9$  Hz), 4.00 (2H, s), 2.83 (2H, t,  $J = 6.6$  Hz), 2.64 (2H, t,  $J = 6.9$  Hz), 2.48 (4H, m), 2.22 (8H, m), 1.96 (2H, quin,  $J = 6.9$  Hz), 1.76 (4H, m).  $^{13}\text{C}$  NMR ( $\text{CDCl}_3$ ):  $\delta$  136.5, 127.6, 126.4, 121.5, 118.9, 113.4, 109.5, 56.5, 55.7, 54.1, 47.9, 45.4, 44.7, 43.9, 28.3, 23.4. MS (ES<sup>+</sup>):  $m/z$  164 ( $M + 2$ , 100%), 329 ( $M + 1$ , 60%).

*N,N*-Dimethyl-3-(3-((3-phenylpropylamino)methyl)-1H-indol-1-yl)propan-1-amine (**30**). Compound **30** was synthesized utilizing general procedure 4, 1-(3-(dimethylamino)propyl)-1H-indole-3-carbaldehyde (**21**) (0.24 g, 1.06 mmol), and phenylpropylamine (0.16 mL, 1.09 mmol), affording *N,N*-dimethyl-3-(3-(3-phenylpropylamino)methyl)-1H-indol-1-yl)propylamine (347 mg, 94%) as an orange oil.  $^1\text{H}$  NMR ( $\text{CDCl}_3$ ):  $\delta$  7.63 (1H, d,  $J = 7.8$  Hz), 7.35 (1H, d,  $J = 8.2$  Hz), 7.18 (6H, m), 7.11 (2H, m), 4.14 (2H, t,  $J = 6.9$  Hz), 3.99 (2H, s), 2.74 (2H, t,  $J = 6.8$  Hz), 2.65 (2H, t,  $J = 7.4$  Hz), 2.24 (2H, t,  $J = 7.0$  Hz), 2.21 (6H, s), 1.95 (2H, quin,  $J = 7.0$  Hz), 1.81 (2H, quin,  $J = 7.7$  Hz).  $^{13}\text{C}$  NMR ( $\text{CDCl}_3$ ):  $\delta$  141.9, 136.4, 128.5, 128.3, 127.5, 126.7, 125.7, 121.6, 119.0, 118.8, 112.4, 109.5, 56.4, 48.6, 45.3, 44.2, 43.9, 33.5, 31.1, 28.2. MS (ES<sup>+</sup>):  $m/z$  175 ( $M + 2$ , 100%), 350 ( $M + 1$ , 80%).

*N*<sup>1</sup>-(Cyclohexylmethyl)-*N*<sup>3</sup>-((1-(3-(dimethylamino)propyl)-1H-indol-3-yl)methyl)propane-1,3-diamine (**31**). Compound **31** was synthesized utilizing general procedure 4, 1-(3-(dimethylamino)propyl)-1H-indole-3-carbaldehyde (**21**) (0.18 g, 0.76 mmol), and *N*-cyclohexyl-1,3-propanediamino-*N*<sup>1</sup>-(cyclohexylmethyl)-*N*<sup>3</sup>-((1-(3-(dimethylamino)propyl)-1H-indol-3-yl)methyl)propane-1,3-diamine (246 mg, 84%) as a yellow oil.  $^1\text{H}$  NMR ( $\text{CDCl}_3$ ):  $\delta$  7.62 (1H, d,  $J = 7.7$  Hz), 7.34 (1H, d,  $J = 7.8$  Hz), 7.20 (1H, m), 7.09 (2H, m), 4.16 (2H, t,

$J = 7.0$  Hz), 3.97 (2H, s), 2.77 (4H, m), 2.21 (8H, m), 1.96 (4H, m), 1.69 (7H, m), 1.16 (4H, m).  $^{13}\text{C}$  NMR ( $\text{CDCl}_3$ ):  $\delta$  136.5, 127.5, 126.7, 121.6, 119.0, 118.8, 112.8, 109.6, 56.9, 56.5, 48.4, 45.8, 45.5, 44.5, 43.9, 40.8, 33.2, 26.0, 25.0. MS (ES<sup>+</sup>):  $m/z$  193 (M + 2, 100%), 385 (M + 1, 30%), 129 (M + 3, 20%).

## ■ ASSOCIATED CONTENT

### Supporting Information

Data parameters for 4, 6, 7, 8, 9, 10, 11, 12, 13, 14, 15, 16, 17, 19, 20, 22, 23, 24, 25, 26, 27, 28, 29, 30, and 31. Dynole, Rhododyn, MiTMAB, Bis-T, Dyngo, and Iminodyn are trademarks of Children's Medical Research Institute and Newcastle Innovation Ltd. Dynole 2–24 and most other dynamin inhibitors described in this paper are available from Abcam Biochemicals (Bristol, UK). This material is available free of charge via the Internet at <http://pubs.acs.org>.

## ■ AUTHOR INFORMATION

### Corresponding Author

\*Phone: +612 4921 6486. Fax: +61 249 215472. E-mail: Adam.McCluskey@newcastle.edu.au.

### Notes

The authors declare the following competing financial interest(s): We have entered into a commercial agreement with Abcam Biochemicals (Bristol, UK) for the supply of our dynamin inhibitors. This includes the compounds listed in this paper.

## ■ ACKNOWLEDGMENTS

This work was supported by grants from the National Health and Medical Research Council (Australia), The Australia Research Council, The Australian Cancer Research Foundation, The Ramaciotti Foundation, The Children's Medical Research Institute, and Newcastle Innovation.

## ■ ABBREVIATIONS USED

CME, clathrin-mediated endocytosis; SVE, synaptic vesicle endocytosis; MiTMAB, myristoyl trimethyl ammonium bromide; OcTMAB, octyl trimethyl ammonium bromide; Bis-T, bis-tyrphostin; RTIL, room temperature ionic liquid; BIM, bisindolylmaleimide; PKC, protein kinase C; PSA, polar surface area; U2OS, human bone osteosarcoma epithelial cells; dynI, dynamin I; dynII, dynamin II; dynIII, dynamin III; FL-dyn I, full length dynamin I; FL-dyn II, full length dynamin II

## ■ REFERENCES

- (1) Ferguson, S. M.; De Camilli, P. Dynamin, a membrane-remodelling GTPase. *Nature Rev. Mol. Cell. Biol.* **2012**, *13*, 75–88.
- (2) Brodin, L.; Low, P.; Shupliakov, O. Sequential steps in clathrin-mediated synaptic vesicle endocytosis. *Curr. Opin. Neurobiol.* **2000**, *10*, 312–320.
- (3) Marks, B.; Stowell, M. H. B.; Vallis, Y.; Mills, I. G.; Gibson, A.; Hopkins, C. R.; McMahon, H. T. GTPase activity of dynamin and resulting conformation change are essential for endocytosis. *Nature* **2001**, *410*, 231–235.
- (4) Hinshaw, J. E. Dynamin and its role in membrane fission. *Annu. Rev. Cell Dev. Biol.* **2000**, *16*, 483–519.
- (5) Hinshaw, J. E.; Schmid, S. L. Dynamin self-assembles into rings suggesting a mechanism for coated vesicle budding. *Nature* **1995**, *374*, 190–192.
- (6) Stowell, M. H.; Marks, B.; Wigge, P.; McMahon, H. T. Nucleotide-dependent conformational changes in dynamin: evidence for a mechanochemical molecular spring. *Nature Cell Biol.* **1999**, *1*, 27–32.

- (7) Anggono, V.; Smillie, K. J.; Graham, M. E.; Valova, V. A.; Cousin, M. A.; Robinson, P. J. Syndapin I is the phosphorylation-regulated dynamin I partner in synaptic vesicle endocytosis. *Nature Neurosci.* **2006**, *9*, 752–760.

- (8) Powell, K. A.; Valova, V. A.; Malladi, C. S.; Jensen, O. N.; Larsen, M. R.; Robinson, P. J. Phosphorylation of dynamin I on Ser-795 by protein kinase C blocks its association with phospholipids. *J. Biol. Chem.* **2000**, *275*, 11610–11617.

- (9) Faelber, K.; Posor, Y.; Gao, S.; Held, M.; Roske, Y.; Schulze, D.; Haucke, V.; Noe, F.; Daumke, O. Crystal structure of nucleotide-free dynamin. *Nature* **2011**, *477*, 556–560.

- (10) Ford, M. G. J.; Jenni, S.; Nunnari, J. The crystal structure of dynamin. *Nature* **2011**, *477*, 561–566.

- (11) Ferguson, S. M.; Brasnjo, G.; Hayashi, M.; Wolfel, M.; Collesi, C.; Giovedi, S.; Raimondi, A.; Gong, L.-W.; Ariel, P.; Paradise, S.; O'Toole, E.; Flavell, R.; Cremona, O.; Miesenbock, G.; Ryan, T. A.; De Camilli, P. A Selective Activity-Dependent Requirement for Dynamin 1 in Synaptic Vesicle Endocytosis. *Science* **2007**, *316*, 570–574.

- (12) Cataldo, A.; Rebeck, G. W.; Ghetti, B.; Hulette, C.; Lippa, C.; Van Broeckhoven, C.; Van Duijn, C.; Cras, P.; Bogdanovic, N.; Bird, T.; Peterhoff, C.; Nixon, R. Endocytic disturbances distinguish among subtypes of Alzheimer's disease and related disorders. *Ann. Neurol.* **2001**, *50*, 661–665.

- (13) Metzler, M.; Legendre-Guillemain, V.; Gan, L.; Chopra, V.; Kwok, A.; McPherson, P. S.; Hayden, M. R. HIP1 functions in clathrin-mediated endocytosis through binding to clathrin and adaptor protein 2. *J. Biol. Chem.* **2001**, *276*, 39271–39276.

- (14) Ong, W. Y.; Kumar, U.; Switzer, R. C.; Sidhu, A.; Suresh, G.; Hu, C. Y.; Patel, S. C. Neurodegeneration in Niemann–Pick type C disease mice. *Exp. Brain Res.* **2001**, *141*, 218–231.

- (15) Sung, J. Y.; Kim, J.; Paik, S. R.; Park, J. H.; Ahn, Y. S.; Chung, K. C. Induction of neuronal cell death by Rab5A-dependent endocytosis of alpha-synuclein. *J. Biol. Chem.* **2001**, *276*, 27441–27448.

- (16) Mercer, J.; Schelhaas, M.; Helenius, A. Virus Entry by Endocytosis. *Annu. Rev. Biochem.* **2010**, *79*, 803–833.

- (17) Veiga, E.; Guttman, J. A.; Bonazzi, M.; Boucrot, E.; Toledo-Arana, A.; Lin, A. E.; Enninga, J.; Pizarro-Cerda, J.; Finlay, B. B.; Kirchhausen, T.; Cossart, P. Invasive and Adherent Bacterial Pathogens Co-Opt Host Clathrin for Infection. *Cell Host Microbe* **2007**, *2*, 340–351.

- (18) Zuechner, S.; Noureddine, M.; Kennerson, M.; Verhoeven, K.; Claeys, K.; De Jonghe, P.; Merory, J.; Oliveira, S. A.; Speer, M. C.; Stenger, J. E.; Walizada, G.; Zhu, D.; Pericak-Vance, M. A.; Nicholson, G.; Timmerman, V.; Vance, J. M. Mutations in the pleckstrin homology domain of dynamin 2 cause dominant intermediate Charcot–Marie–Tooth disease. *Nature Genet.* **2005**, *37*, 289–294.

- (19) Bitoun, M.; Maugenre, S.; Jeannet, P.-Y.; Lacene, E.; Ferrer, X.; Laforet, P.; Martin, J.-J.; Laporte, J.; Lochmueller, H.; Beggs, A. H.; Fardeau, M.; Eymard, B.; Romero, N. B.; Guicheney, P. Mutations in dynamin 2 cause dominant centronuclear myopathy. *Nature Genet.* **2005**, *37*, 1207–1209.

- (20) Zhang, J.; Ding, L.; Holmfeldt, L.; Wu, G.; Heatley, S. L.; Payne-Turner, D.; Easton, J.; Chen, X.; Wang, J.; Rusch, M.; Lu, C.; Chen, S. C.; Wei, L.; Collins-Underwood, J. R.; Ma, J.; Roberts, K. G.; Pounds, S. B.; Ulyanov, A.; Becksfors, J.; Gupta, P.; Huether, R.; Kriwacki, R. W.; Parker, M.; McGoldrick, D. J.; Zhao, D.; Alford, D.; Espy, S.; Bobba, K. C.; Song, G.; Pei, D.; Cheng, C.; Roberts, S.; Barbato, M. I.; Campana, D.; Coustan-Smith, E.; Shurtleff, S. A.; Raimondi, S. C.; Kleppe, M.; Cools, J.; Shimano, K. A.; Hermiston, M. L.; Doulatov, S.; Eppert, K.; Laurenti, E.; Notta, F.; Dick, J. E.; Basso, G.; Hunger, S. P.; Loh, M. L.; Devidas, M.; Wood, B.; Winter, S.; Dunsmore, K. P.; Fulton, R. S.; Fulton, L. L.; Hong, X.; Harris, C. C.; Dooling, D. J.; Ochoa, K.; Johnson, K. J.; Obenaus, J. C.; Evans, W. E.; Pui, C. H.; Naeve, C. W.; Ley, T. J.; Mardis, E. R.; Wilson, R. K.; Downing, J. R.; Mullighan, C. G. The genetic basis of early T-cell precursor acute lymphoblastic leukaemia. *Nature* **2012**, *481*, 157–163.

- (21) Gu, C.; Yaddanapudi, S.; Weins, A.; Osborn, T.; Reiser, J.; Pollak, M.; Hartwig, J.; Sever, S. Direct dynamin-actin interactions regulate the actin cytoskeleton. *EMBO J.* **2010**, *29*, 3593–606.
- (22) Reid, A. T.; Lord, T.; Stranger, S. J.; Roman, S. D.; McCluskey, A.; Robinson, P. J.; Aitken, R. J.; Nixon, B. Dynamin regulates specific membrane fusion events necessary for acrosomal exocytosis in mouse spermatozoa. *J. Biol. Chem.* **2012**, *287*, 37659–37672.
- (23) Chircop, M.; Perera, S.; Mariana, A.; Lau, H.; Ma, M. P. C.; Gilbert, J.; Jones, N. C.; Gordon, C. P.; Young, K. A.; Morokoff, A.; Sakoff, J.; O'Brien, T. J.; McCluskey, A.; Robinson, P. J. Inhibition of dynamin by Dynole 34–2 Induces Cell Death Following Cytokinesis Failure in Cancer Cells. *Mol. Cancer Ther.* **2011**, *10*, 1553–1562.
- (24) Hill, T. A.; Odell, L. R.; Quan, A.; Abagyan, R.; Ferguson, G.; Robinson, P. J.; McCluskey, A. Long chain amines and long chain ammonium salts as novel inhibitors of dynamin GTPase activity. *Bioorg. Med. Chem. Lett.* **2004**, *14*, 3275–3278.
- (25) Quan, A.; McGeachie, A. B.; Keating, D. J.; van Dam, E. M.; Rusak, J.; Chau, N.; Malladi, C. S.; Chen, C.; McCluskey, A.; Cousin, M. A.; Robinson, P. J. Myristyl trimethyl ammonium bromide and octadecyl trimethyl ammonium bromide are surface-active small molecule dynamin inhibitors that block endocytosis mediated by dynamin I or dynamin II. *Mol. Pharmacol.* **2007**, *72*, 1425–1439.
- (26) Hill, T.; Odell, L. R.; Edwards, J. K.; Graham, M. E.; McGeachie, A. B.; Rusak, J.; Quan, A.; Abagyan, R.; Scott, J. L.; Robinson, P. J.; McCluskey, A. Small molecule inhibitors of dynamin I GTPase activity: development of dimeric tyrphostins. *J. Med. Chem.* **2005**, *48*, 7781–7788.
- (27) Odell, L. R.; Chau, N.; Mariana, A.; Graham, M. E.; Robinson, P. J.; McCluskey, A. Azido and diazirinyl analogues of bis-tyrphostin as asymmetrical inhibitors of dynamin GTPase. *ChemMedChem.* **2009**, *4*, 1182–1188.
- (28) Zhang, J.; Lawrance, G. A.; Chau, N.; Robinson, P. J.; McCluskey, A. From Spanish fly to room-temperature ionic liquids (RTILs): synthesis, thermal stability and inhibition of dynamin I GTPase by a novel class of RTILs. *New J. Chem.* **2008**, *32*, 28–36.
- (29) Hill, T. A.; Mariana, A.; Gordon, C. P.; Odell, L. R.; Robertson, M. J.; McGeachie, A. B.; Chau, N.; Daniel, J. A.; Gorgani, N. N.; Robinson, P. J.; McCluskey, A. Iminochromene inhibitors of dynamins I and II GTPase activity and endocytosis. *J. Med. Chem.* **2010**, *53*, 4094–4102.
- (30) Odell, L. R.; Howan, D.; Gordon, C. P.; Robertson, M. J.; Chau, N.; Mariana, A.; Whiting, A. E.; Abagyan, R.; Daniel, J. A.; Gorgani, N. N.; Robinson, P. J.; McCluskey, A. The pthaladyns: GTP competitive inhibitors of dynamin I and II GTPase derived from virtual screening. *J. Med. Chem.* **2010**, *53*, 5267–5280.
- (31) Harper, C. B.; Martin, S.; Nguyen, T. H.; Daniels, S. J.; Lavidis, N. A.; Popoff, M. R.; Hadzic, G.; Mariana, A.; Chau, N.; McCluskey, A.; Robinson, P. J.; Meunier, F. A. Dynamin Inhibition Blocks Botulinum Neurotoxin Type A Endocytosis in Neurons and Delays Botulism. *J. Biol. Chem.* **2011**, *286*, 35966–35976.
- (32) Robertson, M. J.; Hadzic, G.; Ambrus, J.; Pomá, D. Y.; Hyde, E.; Whiting, A.; Mariana, A.; von Kleist, L.; Chau, N.; Haucke, V.; Robinson, P. J.; McCluskey, A. The Rhodadyns, a New Class of Small Molecule Inhibitors of dynamin GTPase Activity. *ACS Med. Chem. Lett.* **2012**, *3*, 352–356.
- (33) Hill, T. A.; Gordon, C. P.; McGeachie, A. B.; Venn-Brown, B.; Odell, L. R.; Chau, N.; Quan, A.; Mariana, A.; Sakoff, J. A.; Chircop, M.; Robinson, P. J.; McCluskey, A. Inhibition of dynamin mediated endocytosis by the dynoles—synthesis and functional activity of a family of indoles. *J. Med. Chem.* **2009**, *52*, 3762–3773.
- (34) Ali, A.; Bliese, M.; Rasmussen, J.-A. M.; Sargent, R. M.; Saubern, S.; Sawutz, D. G.; Wilkie, J. S.; Winkler, D. A.; Winzenberg, K. N.; Woodgate, R. C. J. Discovery of (Z)-2-phenyl-3-(1H-pyrrol-2-yl)acrylonitrile derivatives active against *Haemonchus contortus* and *Ctenocephalides felis* (cat flea). *Bioorg. Med. Chem. Lett.* **2007**, *17*, 993–997.
- (35) Biradar, J. S.; Sasidhar, B. S. Solvent-free, microwave assisted Knoevenagel condensation of novel 2,5-disubstituted indole analogues and their biological evaluation. *Eur. J. Med. Chem.* **2011**, *46*, 6112–6118.
- (36) Correa, W. H.; Edwards, J. K.; McCluskey, A.; McKinnon, I.; Scott, J. L. A thermodynamic investigation of solvent-free reactions. *Green Chem.* **2003**, *5*, 30–33.
- (37) Tarleton, M.; Gilbert, J.; Robertson, M. J.; McCluskey, A.; Sakoff, J. A. Library synthesis and cytotoxicity of a family of 2-phenylbutene-3-nitriles. *MedChemCommun* **2010**, *2*, 31–37.
- (38) Hayashi, Y.; Toyoshima, M.; Gotoh, H.; Ishikawa, H. Diphenylprolinol silyl ether catalysis in an asymmetric formal carbo [3 + 3] cycloaddition reaction via a domino Michael/Knoevenagel condensation. *Org. Lett.* **2009**, *11*, 45–48.
- (39) Jautze, S.; Peters, R. Asymmetric Michael Additions of  $\alpha$ -Cyanoacetates. *Synthesis* **2010**, 365–388.
- (40) McCluskey, A.; Robinson, P. J.; Hill, T.; Scott, J. L.; Edwards, J. K. Green chemistry approaches to the Knoevenagel condensation: comparison of ethanol, water and solvent free (dry grind) approaches. *Tetrahedron Lett.* **2002**, *43*, 3117–3120.
- (41) Sonawane, Y. A.; Phadtare, S. B.; Borse, B. N.; Jagtap, A. R.; Shankarling, G. S. Synthesis of diphenylamine-based novel fluorescent styryl colorants by Knoevenagel condensation using a conventional method, biocatalyst, and deep eutectic solvent. *Org. Lett.* **2010**, *12*, 1456–1459.
- (42) Baxendale, I. R.; Pitts, M. R. Microwave flow chemistry: the next evolutionary step in synthetic chemistry? *Chim. Oggi* **2006**, *24*, 41–45.
- (43) Colombo, M.; Peretto, I. Chemistry strategies in early drug discovery: an overview of recent trends. *Drug Discovery Today* **2008**, *13*, 677–684.
- (44) Hessel, V. Novel Process Windows—Gate to Maximizing Process Intensification via Flow Chemistry. *Chem. Eng. Technol.* **2009**, *32*, 1655–1681.
- (45) Tarleton, M.; McCluskey, A. A flow chemistry route to 2-phenyl-3-(1H-pyrrol-2-yl)propan-1-amines. *Tetrahedron Lett.* **2011**, *52*, 1583–1586.
- (46) Tarleton, M.; Young, K. A.; Unicomb, E.; McCluskey, S. N.; Robertson, M. J.; Gordon, C. P.; McCluskey, A. A flow chemistry approach to norcantharidin analogues. *Lett. Drug Des. Dis.* **2011**, *8*, 568–574.
- (47) Clapham, B.; Wilson, N. S.; Michmerhuizen, M. J.; Blanchard, D. P.; Dingle, D. M.; Nemcek, T. A.; Pan, J. Y.; Sauer, D. R. Construction and validation of an automated flow hydrogenation instrument for application in high-throughput organic chemistry. *J. Comb. Chem.* **2008**, *10*, 88–93.
- (48) Lou, S.; Dai, P.; Schaus, S. E. Asymmetric Mannich reaction of dicarbonyl compounds with  $\alpha$ -amido sulfones catalyzed by cinchona alkaloids and synthesis of chiral dihydropyrimidones. *J. Org. Chem.* **2007**, *72*, 9998–10008.
- (49) Franckevicius, V.; Knudsen, K. R.; Ladlow, M.; Longbottom, D. A.; Ley, S. V. Practical synthesis of (S)-pyrrolidin-2-yl-1H-tetrazole, incorporating efficient protecting group removal by flow-reactor hydrogenolysis. *Synlett* **2006**, 889–892.
- (50) Horvath, H. H.; Papp, G.; Csajagi, C.; Joo, F. Selective catalytic hydrogenations in a microfluidics-based high throughput flow reactor on ion-exchange supported transition metal complexes: A modular approach to the heterogenization of soluble complex catalysts. *Catal. Commun.* **2007**, *8*, 442–446.
- (51) Jones, R. V.; Godorhazy, L.; Varga, N.; Szalay, D.; Urge, L.; Darvas, F. Continuous-flow high pressure hydrogenation reactor for optimization and high-throughput synthesis. *J. Comb. Chem.* **2006**, *8*, 110–116.
- (52) Szollosi, G.; Herman, B.; Fulop, F.; Bartok, M. Continuous enantioselective hydrogenation of activated ketones on a Pt-CD chiral catalyst: use of H-cube reactor system. *React. Kinet. Catal. Lett.* **2006**, *88*, 391–398.
- (53) Dijkstra, G.; Kruizinga, W. H.; Kellogg, R. M. An assessment of the causes of the “cesium effect”. *J. Org. Chem.* **1987**, *52*, 4230–4234.
- (54) Warnock, D. E.; Baba, T.; Schmid, S. L. Ubiquitously expressed dynamin-II has a higher intrinsic GTPase activity and a greater

propensity for self-assembly than neuronal dynamin-I. *Mol. Biol. Cell* **1997**, *8*, 2553–2562.

(55) van der Blik, A. M.; Redelmeier, T. E.; Damke, H.; Tisdale, E. J.; Meyerowitz, E. M.; Schmid, S. L. Mutations in human dynamin block an intermediate stage in coated vesicle formation. *J. Cell Biol.* **1993**, *122*, 553–563.

(56) Maruoka, N.; Murata, T.; Omata, N.; Takashima, Y.; Tani, H.; Yonekura, Y.; Fujibayashi, Y.; Wada, Y. Effects of chlorpromazine on plasma membrane permeability and fluidity in the rat brain: a dynamic positron autoradiography and fluorescence polarization study. *Prog. Neuropsychopharmacol. Biol. Psychiatry* **2007**, *31*, 178–186.